

NexTech Materials, Ltd  
404 Enterprise Drive  
Lewis Center, OH 43035

+1-614-842-6606  
FAX +1-614-842-6607  
[www.nextechmaterials.com](http://www.nextechmaterials.com)  
[www.fuelcellmaterials.com](http://www.fuelcellmaterials.com)

---

## FINAL REPORT

### *Tailored Core Shell Cathode Powders for Solid Oxide Fuel Cells*

U.S. Department of Energy Contract No. DE-SC0011849

**Performing Organization:** NexTech Materials, Ltd.

**Principal Investigator:** Scott L. Swartz, Ph.D.

**Period of Performance:** June 9, 2014 through March 8, 2015

**Date:** March 23, 2015

## **TABLE OF CONTENTS**

Table of Contents .....	3
Executive Summary .....	4
Introduction .....	5
Results and Discussion .....	6
Literature Review .....	6
Sample Preparation and Characterization .....	7
Baseline Cathodes .....	7
Milling Method .....	7
Precipitation Method .....	9
Hetero-Coagulation Method .....	13
Electrochemical Testing .....	15
EIS Measurements .....	15
Single-Cell SOFC Testing .....	20
Summary And Conclusions .....	28
Literature Cited .....	29
Appendix A. Literature Survey .....	30

## **EXECUTIVE SUMMARY**

In this Phase I SBIR project, a “core-shell” composite cathode approach was evaluated for improving SOFC performance and reducing degradation of lanthanum strontium cobalt ferrite (LSCF) cathode materials, following previous successful demonstrations of infiltration approaches for achieving the same goals. The intent was to establish core-shell cathode powders that enabled high performance to be obtained with “drop-in” process capability for SOFC manufacturing (i.e., rather than adding an infiltration step to the SOFC manufacturing process).

Milling, precipitation and hetero-coagulation methods were evaluated for making core-shell composite cathode powders comprised of coarse LSCF “core” particles and nanoscale “shell” particles of lanthanum strontium manganite (LSM) or praseodymium strontium manganite (PSM). Precipitation and hetero-coagulation methods were successful for obtaining the targeted core-shell morphology, although perfect coverage of the LSCF core particles by the LSM and PSM particles was not obtained.

Electrochemical characterization of core-shell cathode powders and conventional (baseline) cathode powders was performed via electrochemical impedance spectroscopy (EIS) half-cell measurements and single-cell SOFC testing. Reliable EIS testing methods were established, which enabled comparative area-specific resistance measurements to be obtained. A single-cell SOFC testing approach also was established that enabled cathode resistance to be separated from overall cell resistance, and for cathode degradation to be separated from overall cell degradation. The results of these EIS and SOFC tests conclusively determined that the core-shell cathode powders resulted in significant lowering of performance, compared to the baseline cathodes.

Based on the results of this project, it was concluded that the core-shell cathode approach did not warrant further investigation.

## INTRODUCTION

Contemporary solid oxide fuel cells, either anode or electrolyte supported, utilize cathode materials based on perovskite structured lanthanum manganites, ferrites and cobaltites, such as lanthanum strontium manganite (LSM) and lanthanum strontium cobalt ferrite (LSCF). A wide body of recent research work, including work sponsored by DOE's Solid State Energy Conversion Alliance (SECA) program, has confirmed the advantages of making cathodes with composite (core-shell) microstructures [1-37]. These approaches typically involve infiltration of catalyst precursors into pre-formed porous cathode or electrolyte coatings. After annealing, surfaces of the original cathode or electrolyte particles are decorated with nanoscopic particles of the targeted catalytically active material. This approach enables the use of catalytically active cathode materials, including  $(La_{0.6}Sr_{0.4})CoO_{3-\delta}$  [8-10],  $(Sm_{0.5}Sr_{0.5})CoO_{3-\delta}$  [11-15], and other materials [16-17] that otherwise could not be used due to thermal expansion mismatches, chemical reactivity issues, and/or poor long-term stability. The approach also has been employed by NexTech [38] and others [24-37] to add ceria electrolyte material into cathodes, with significant performance enhancements demonstrated. Recently, infiltration approaches have been used to stabilize the performance of LSCF cathodes, by coating LSCF particle surfaces with nanoscale LSM [4-6] or lanthanum/calcium co-doped ceria [7] particles. This stabilization was enabled by preventing diffusion of lanthanum and strontium species from the bulk to the active surface sites.

In this Phase I SBIR project, NexTech Materials performed comparative study of compositions and processing methods for solid oxide fuel cell (SOFC) cathode powders with core-shell morphologies (see Figure 1). This project leveraged results of SECA's research and aimed to deliver high performance cathode materials with "drop-in" process capability to SOFC manufacturers.

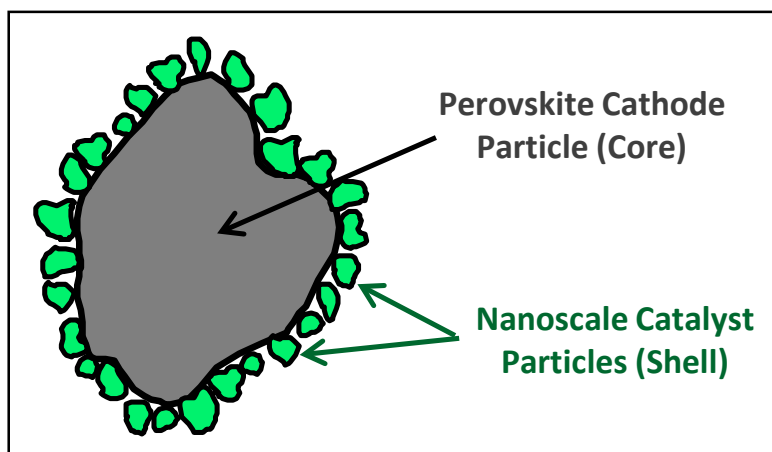


**Figure 1.** Core-shell microstructure achieved with infiltration processes.

## RESULTS AND DISCUSSION

Exhibit 1 provides an assessment of the Phase 1 project results against the originally proposed objectives. Detailed presentation and discussion of results are provided in sections that follow.

### **Exhibit 1. Assessment of Phase 1 Progress.**

**Objective:** Establish processes for making core-shell cathode powders with particle size and surface area that are amenable to conventional screen printing deposition processes.

**Phase 1 Results.** Multiple conventional and core-shell cathode powders were prepared and characterized. These powders were prepared with micron-scale particle sizes and surface areas of less than 15 m<sup>2</sup>/gram, making them compatible with screen printing processes.

**Objective:** Evaluate the effectiveness of candidate core-shell cathodes using electrochemical impedance spectroscopy on half cells.

**Phase 1 Results.** Sample preparation and electrochemical impedance spectroscopy (EIS) testing methods were established, and multiple EIS tests were completed. Consistent results were obtained, which confirmed that core-shell cathodes were inferior to their conventional counterparts.

**Objective:** Evaluate performance and short-term durability of at least four down-selected core-shell cathode formulations via single-cell and short-stack stack testing.

**Phase 1 Results.** Single-cell SOFC testing methods were established such that performance and durability of large-area cells to be assessed and cathode resistances could be separated and quantified. Again, conventional cathodes outperformed the core-shell materials.

**Objective:** Perform a cost-benefit analysis of the core-shell cathode materials.

**Phase 1 Results.** All of the processes that were pursued in this project were scalable at high volumes. However, this task was not warranted based on the results obtained.

## Literature Review

NexTech completed a review of technical literature related to core-shell SOFC cathodes, and this review is summarized in Appendix A. The literature review did not find articles that suggested any changes to our originally proposed core-shell powder synthesis methods. However, several articles were identified that provided alternative compositions and synthesis methods that could have been considered if the project continued into a second phase. In addition, following a suggestion by Dr. Briggs White of NETL, the literature search was expanded to include core-shell electrode materials for lithium ion batteries. Several very recent technical articles were identified, which indicated that lithium ion battery cathode materials also are greatly improved when made with core-shell morphologies.

### Sample Preparation and Characterization

Constituent powders for core-shell cathode materials were made and characterized by particle size and surface area measurements (see Table 1). These powders were used in the as-prepared state for baseline single-phase (LSCF) cathodes, as precursors to composite (LSCF/GDC) cathodes, and as precursors to core-shell cathode powders. Synthesis and characterization of the various baseline and core-shell cathode powders are described below.

<b>Table 1.</b> Characterization of component cathode materials.		
<b>Material</b>	<b>Particle Size (<math>D_{50}</math>)</b>	<b>Surface Area</b>
$(La_{0.60}Sr_{0.40})_{0.95}(Co_{0.20}Fe_{0.8})O_{3-\delta}$ (LSCF-coarse)	1.0 microns	5.1 m <sup>2</sup> /gram
$(La_{0.60}Sr_{0.40})_{0.95}(Co_{0.20}Fe_{0.8})O_{3-\delta}$ (LSCF-nano)	0.4 microns	21.1 m <sup>2</sup> /gram
$(La_{0.60}Sr_{0.20})_{0.95}MnO_{3-\delta}$ (LSM-nano)	0.3 microns	19.2 m <sup>2</sup> /gram
$(Ce_{0.90}Gd_{0.10})O_{2.95}$ (GDC-coarse)	0.2 microns	6.4 m <sup>2</sup> /gram
$(Ce_{0.90}Gd_{0.10})O_{2.95}$ (GDC-nano)	0.2 microns	34.6 m <sup>2</sup> /gram

### Baseline Cathodes

Two baseline cathode powders were prepared and formulated into screen printing inks, including single-phase (LSCF) and composite (LSCF/GDC) cathodes. The LSCF ink was prepared from the coarse LSCF material in Table 1, and LSCF/GDC (70/30 vol%) inks were made from the coarse LSCF and GDC materials in Table 1. Composite formulations based on NexTech's patented lanthanum strontium zinc ferrite (LSZF) perovskite composition also were prepared for baseline testing.

### Milling Method

This core-shell powder synthesis approach involved milling of coarse LSCF powder and nanoscale LSM (and/or GDC) powders, with the intent of having the nanoscale (LSM and GDC) particles decorating the surface of coarse LSCF particles. This approach previously had been employed at NexTech for making nano-composite NiO/YSZ anode materials (U.S. Patent No. 7,595,127). Surface area measurements were made (Table 2), and these data were consistent with expectations based on surface areas of constituent LSCF, LSM and GDC powders. A milled core-shell powder (LSCF / LSM-GDC) was selected for analysis by transmission electron microscopy (TEM), in conjunction with energy dispersive spectroscopy (EDS). This formulation was designed to have a core of LSCF and a shell comprised of LSM and GDC. TEM results (shown in Figure 2) clearly

show that the targeted core-shell morphology was not achieved. The EDS analysis confirmed that small GDC particles were attached to larger LSM and LSCF particles, but that the LSM and LSCF particles were separated from each other. For this reason, the milling approach was abandoned.

**Table 2.** Compositions and Surface areas of core-shell powders (milling method).

Cathode Composition			Surface Area (m <sup>2</sup> /gram)
Core	Shell	Volume Ratio	
LSCF	GDC-nano	70/30	15.4
LSCF	LSCF-nano / GDC-nano (50/50 vol%)	70/30	12.0
LSCF	LSM-nano	70/30	9.4
LSCF	LSM-nano / GDC-nano (50/50 vol%)	70/30	11.7

LSCF =  $(La_{0.60}Sr_{0.40})_{0.95}(Co_{0.20}Fe_{0.80})O_{3-\delta}$   
LSM =  $(La_{0.80}Sr_{0.20})_{0.95}MnO_{3-\delta}$   
GDC =  $(Ce_{0.90}Gd_{0.10})O_{1.95}$

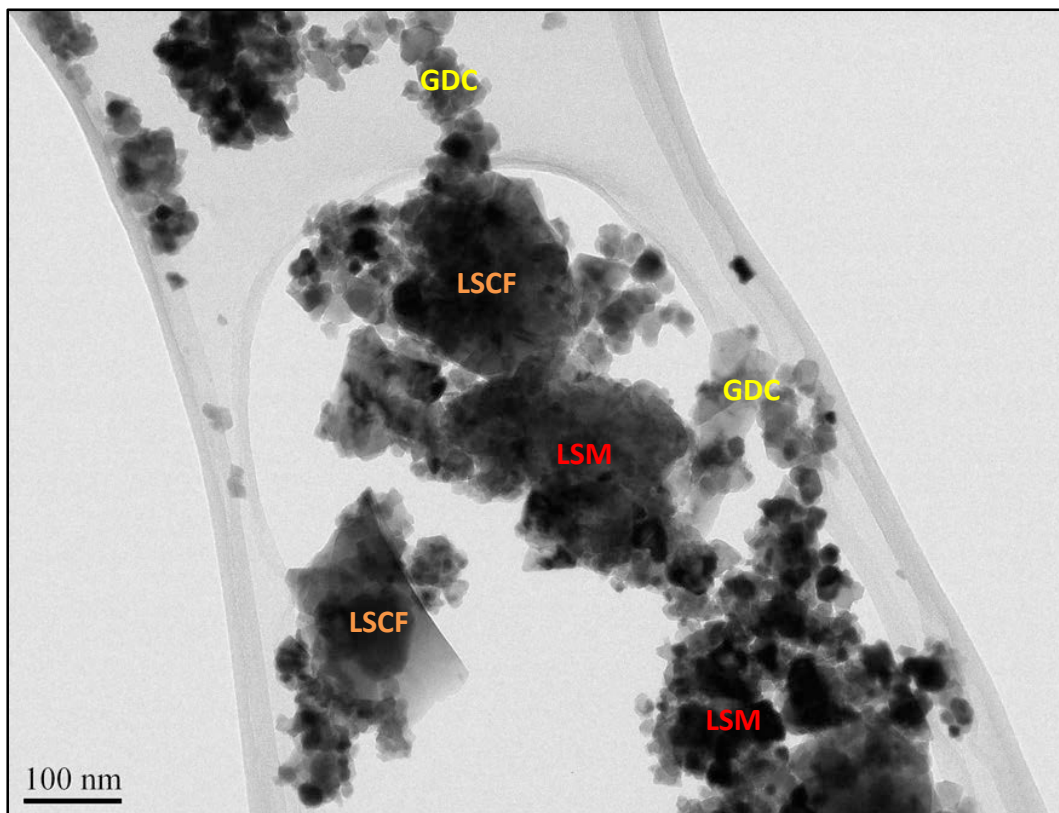


**Figure 2.** TEM micrograph of milled LSCF/LSM-GDC powder.

## **Precipitation Method**

This core-shell powder synthesis approach involved deposition of nanoscale particles of lanthanum strontium manganite ( $\text{La}_{0.60}\text{Sr}_{0.20})_{0.95}\text{MnO}_{3-\delta}$  or LSM) or praseodymium strontium manganite ( $\text{Pr}_{0.80}\text{Sr}_{0.20})_{0.95}\text{MnO}_{3-\delta}$  or PSM) onto coarse LSCF particles. Aqueous suspensions of LSCF powder were prepared and mixed with aqueous solutions of LSM or PSM precursor salts, and the LSM or PSM shells particles were precipitated onto the LSCF particle surfaces by addition of a basic ammonium carbonate solution. The resulting core-shell powders then were calcined in order to crystallize the LSM or PSM shell particles into the targeted perovskite crystal structure. Calcination temperatures of 850 to 1100°C were evaluated, with characterization by surface area measurements (Table 3) and by x-ray diffraction analyses (Figures 3 through 6). These data are summarized below.

**Table 3.** Compositions and Surface areas of core-shell powders (precipitation method).

Formulation	Calcination Temperature	Surface Area (m <sup>2</sup> /gram)
60 vol% LSCF / 40 vol% LSM	900°C	5.6
	1000°C.	3.4
	1100°C	1.7
80 vol% LSCF / 20 vol% LSM	850°C	5.1
	900°C	4.0
	1000°C	2.4
	1100°C	1.4
60 vol% LSCF / 40 vol% PSM	900°C	4.2
	1000°C	3.1
	1100°C	1.3
80 vol% LSCF / 20 vol% PSM	900°C	2.8
	1000°C	2.1
	1100°C	1.2
LSCF = $(\text{La}_{0.60}\text{Sr}_{0.40})_{0.95}(\text{Co}_{0.20}\text{Fe}_{0.80})\text{O}_{3-\delta}$ LSM = $(\text{La}_{0.80}\text{Sr}_{0.20})_{0.95}\text{MnO}_{3-\delta}$ PSM = $(\text{Pr}_{0.60}\text{Sr}_{0.40})_{0.95}\text{MnO}_{3-\delta}$		

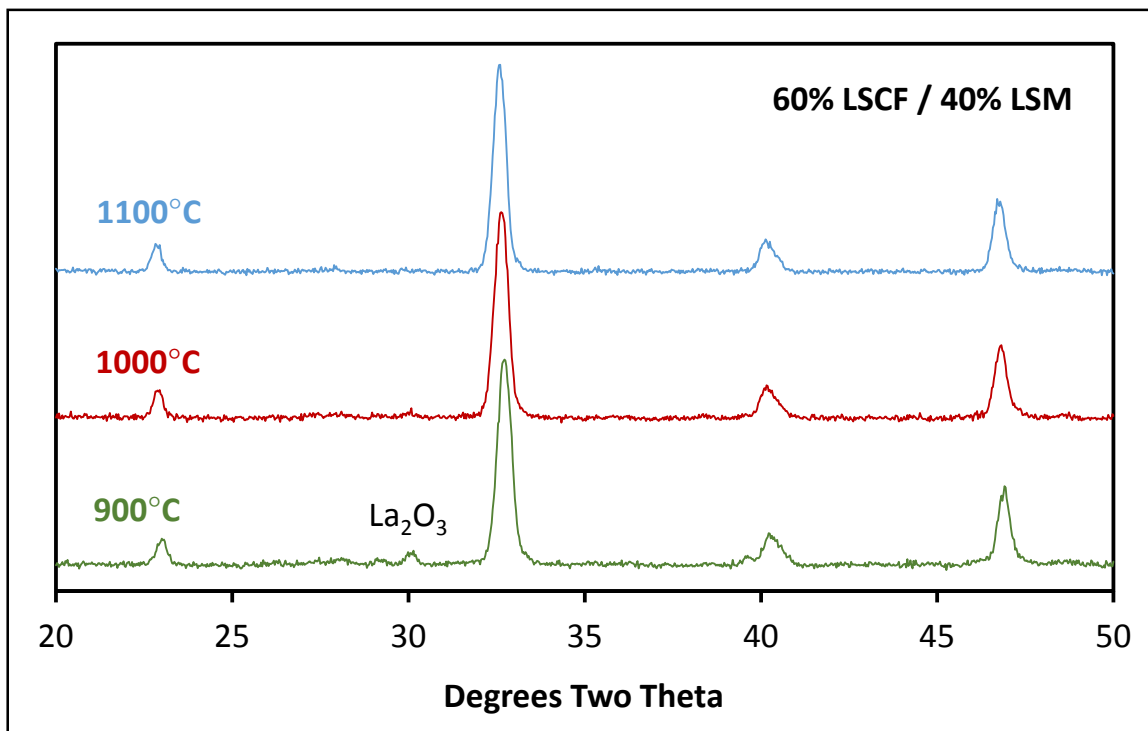


**Figure 3.** XRD patterns of core-shell LSCF/LSM (60/40) powders prepared by the precipitation method after calcination at 900, 1000 and 1100°C for three hours.

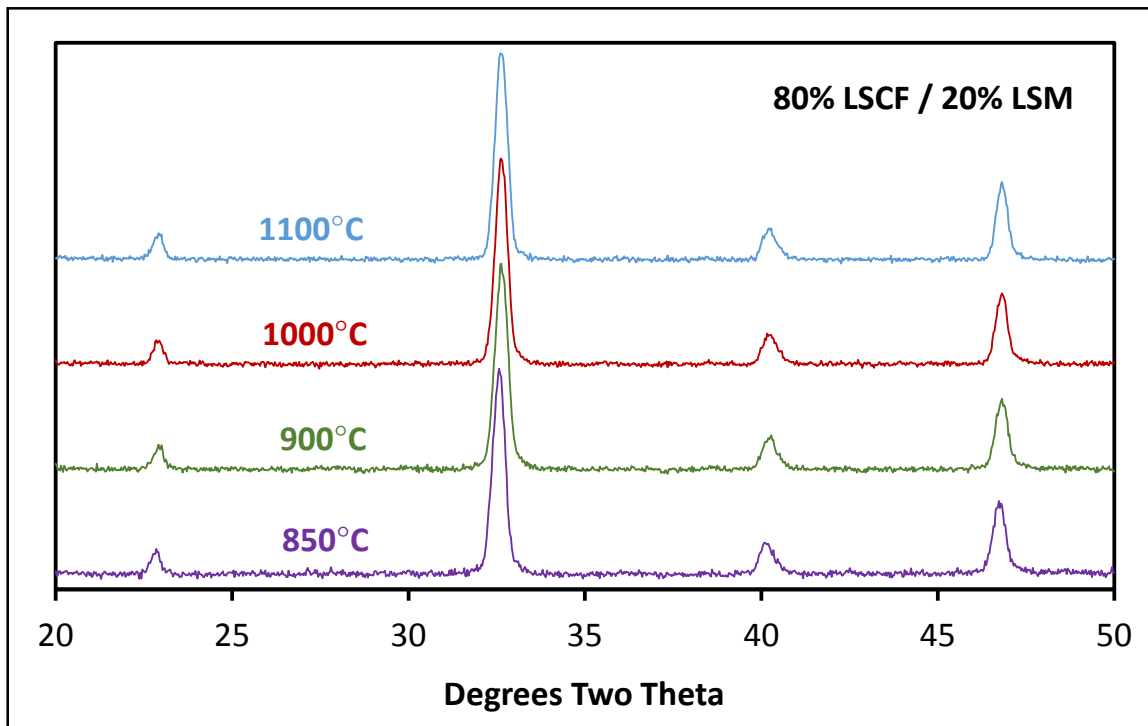


**Figure 4.** XRD patterns of core-shell LSCF/LSM (80/20) powders prepared by the precipitation method after calcination at 900, 1000 and 1100°C for three hours.

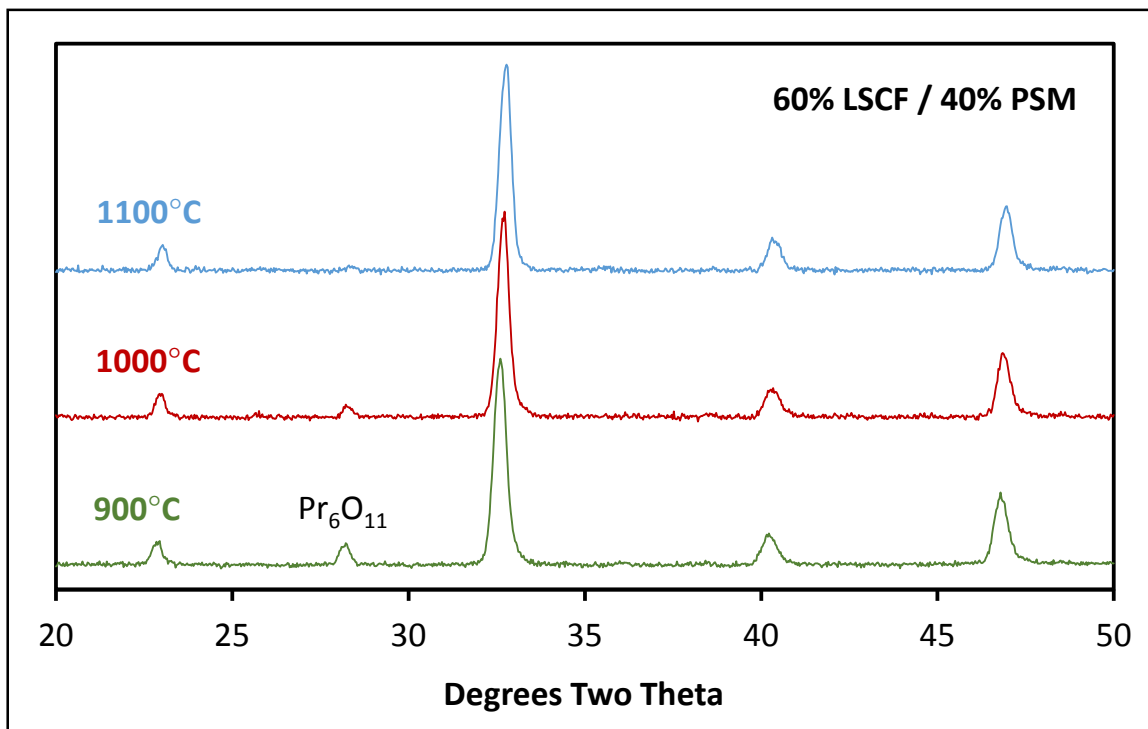


**Figure 5.** XRD of core-shell LSCF/PSM (60/40) powders prepared by the precipitation method after calcination at 900, 1000 and 1100°C for three hours.

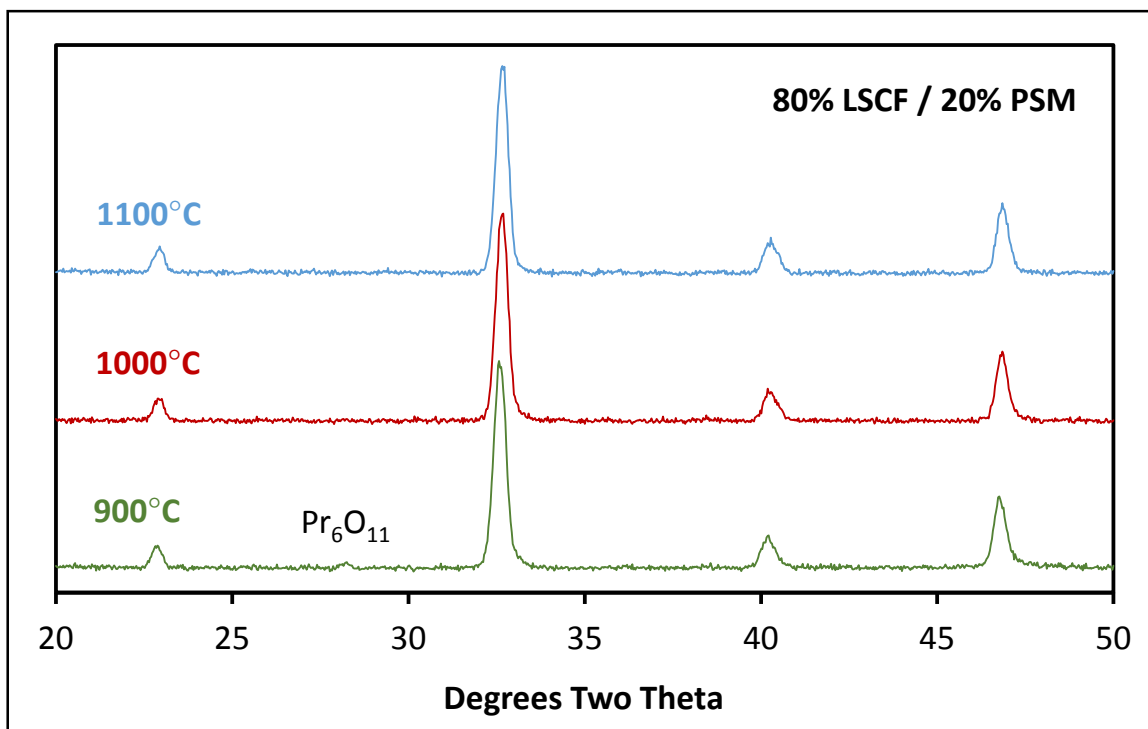


**Figure 6.** XRD patterns of core-shell LSCF/PSM (80/20) powders prepared by the precipitation method after calcination at 900, 1000 and 1100°C for three hours.

- ❖ Surface areas of precipitated core-shell powders of the four compositions decreased with increasing calcination temperature, which is exactly as expected. However, the surface areas were lower than expected, ranging from 3-6 m<sup>2</sup>/gram for samples calcined at 850 to 900°C, and from 1-3 m<sup>2</sup>/gram.
- ❖ For the LSCF/LSM (60/40) composition (Figure 3), XRD analysis suggested a single perovskite phase, with a La<sub>2</sub>O<sub>3</sub> impurity phase present in powder calcined at the lowest temperature (900°C). This La<sub>2</sub>O<sub>3</sub> second phase was absent in powders calcined at 1000 and 1100°C. For the LSCF/LSM (80/20) composition (Figure 4), XRD indicated phase-pure perovskite at all calcination temperatures.
- ❖ For the LSCF/PSM (60/40) composition (Figure 5), XRD suggested a single perovskite phase, with a small amount of Pr<sub>6</sub>O<sub>11</sub> second phase in powder calcined at 900 and 1000°C. This Pr<sub>6</sub>O<sub>11</sub> phase was absent in powder calcined at 1100°C. For the LSCF/LSM (60/40) composition (Figure 6), a single perovskite phase was evident, with a small amount of Pr<sub>6</sub>O<sub>11</sub> present in powder calcined at the lowest temperature (900°C). This Pr<sub>6</sub>O<sub>11</sub> phase was absent in powders calcined at 1000 and 1100°C.

It should be noted that theoretical XRD peak positions for LSCF, LSM and PSM phases are extremely close. Thus, it could not be conclusively determined whether the targeted core-shell morphologies were obtained or whether perovskite solid solutions were formed during calcination. Thus, TEM/EDS analyses were performed on the LSCF/LSM (80/20) powder (calcined at 900°C), and these results are shown in Figure 7. This formulation was designed to have a core of LSCF and a shell of LSM. The TEM results clearly show that the targeted core-shell morphology was achieved, but that the core LSCF particle surfaces were not perfectly covered by the nanoscale LSM shell particles. EDS analysis confirmed that the large (core) particle was LSCF and that the small (shell) particles were LSM.

Based on these results, precipitated core-shell powders were further processed into inks for cathode performance evaluation. The precipitated LSCF/LSM (80/20) feedstock was calcined at 900°C, and then ball milled for a short time. The intent of the milling step was to break up calcined agglomerates (ideally without destroying the core-shell morphology). Average particle size (d<sub>50</sub>) was 2.0 microns after calcination, and the milling step reduced the particle size to 1.1 microns. This is very close to the particle size of the starting LSCF powder (1.0 microns), which suggests that the milling step successfully served its intended purpose. This core-shell LSCF/LSM powder then was evaluated by electrochemical testing (which is described later in this report).

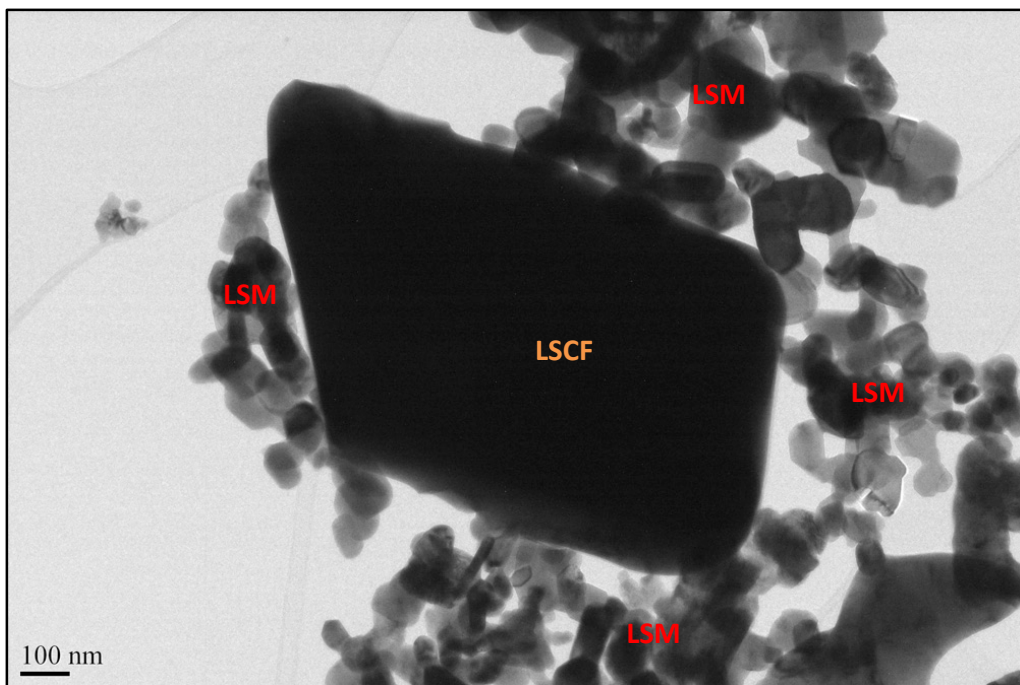


**Figure 7.** TEM micrograph of precipitated LSCF/LSM core-shell powder (calcined at 900°C).

### Hetero-Coagulation Method

In addition to the above (originally proposed) core-shell powder synthesis methods, an alternative method was conceived and evaluated. This method is based on hetero-coagulation and involves the addition of surfactants to coarse LSCF and nanoscale LSM powders prior to mixing. Through proper selection of surfactants, the LSCF and LSM particles can be made to have opposite surface charges in aqueous suspension, and thus be attracted to one another. This approach previously has been used to make aluminum oxide based nano-composite core-shell particles, an example of which is shown in Figure 8. Two synthesis trials were executed for making core shell LSCF/LSM powders, with 80/20 and 70/30 volume ratios. Particle size and surface area information on starting LSCF and LSM powders for these hetero-coagulated powders is provided in Table 4.

**Table 4.** Characterization data on LSCF and LSM powders for hetero-coagulation trials.

Composition	LSCF/LSM (80/20)	LSCF/LSM (70/30)
LSCF Particle Size (d <sub>50</sub> , microns)	1.2	3.1
LSCF Surface Area (m <sup>2</sup> /gram)	3.9	4.0
LSM Particle Size (d <sub>50</sub> , microns)	0.30	0.19
LSM Surface Area (m <sup>2</sup> /gram)	19.2	38.6

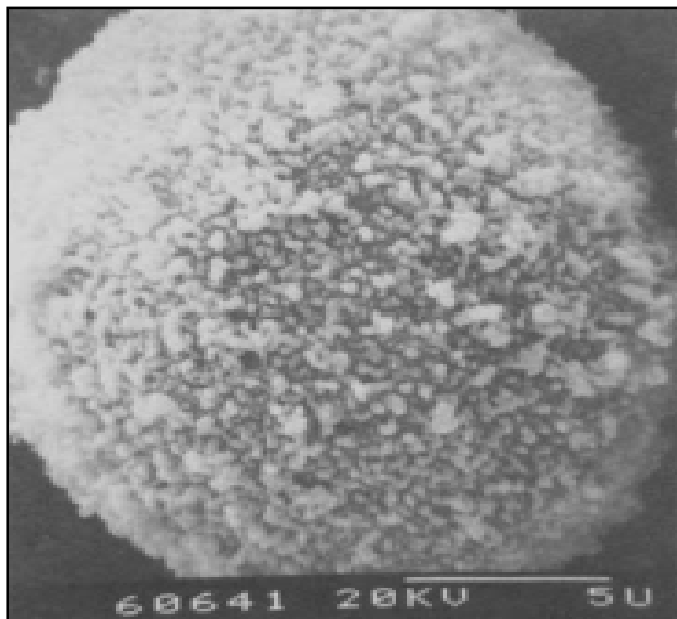


**Figure 2.** SEM micrograph of alumina spheres coated with alumina particles using the hetero-coagulation method<sup>[38]</sup>.

The hetero-coagulation synthesis experiments were moderately successful, as shown by SEM micrographs in Figure 9 and 10. The powder morphologies consisted of nanoscale LSM particles attached to the surfaces of coarse LSCF particles. However, the surface coverage was not perfect and there was evidence of agglomerated nanoscale LSM particles.

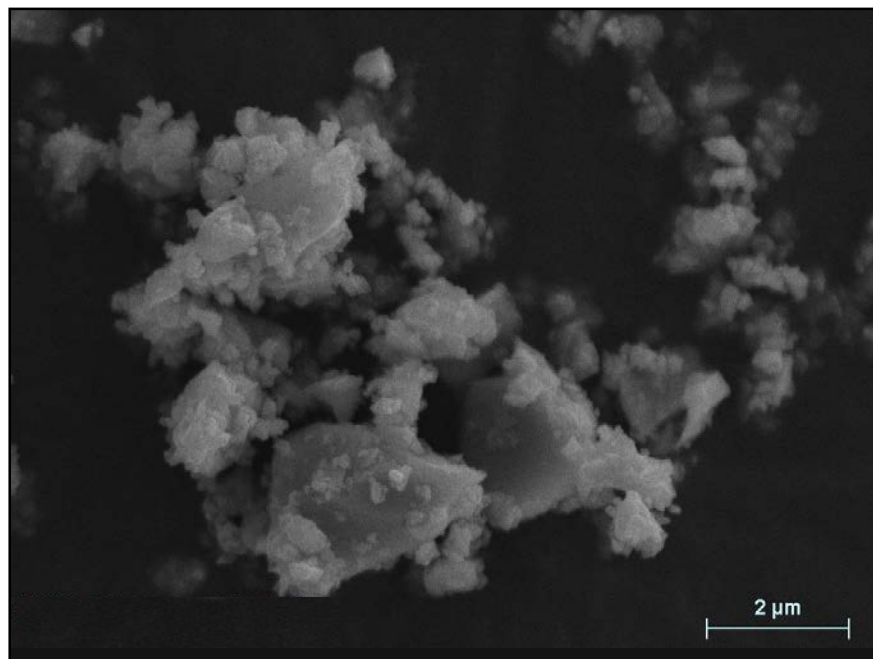


**Figure 9.** SEM micrograph of hetero-coagulated LSCF/LSM (80/20) powder.

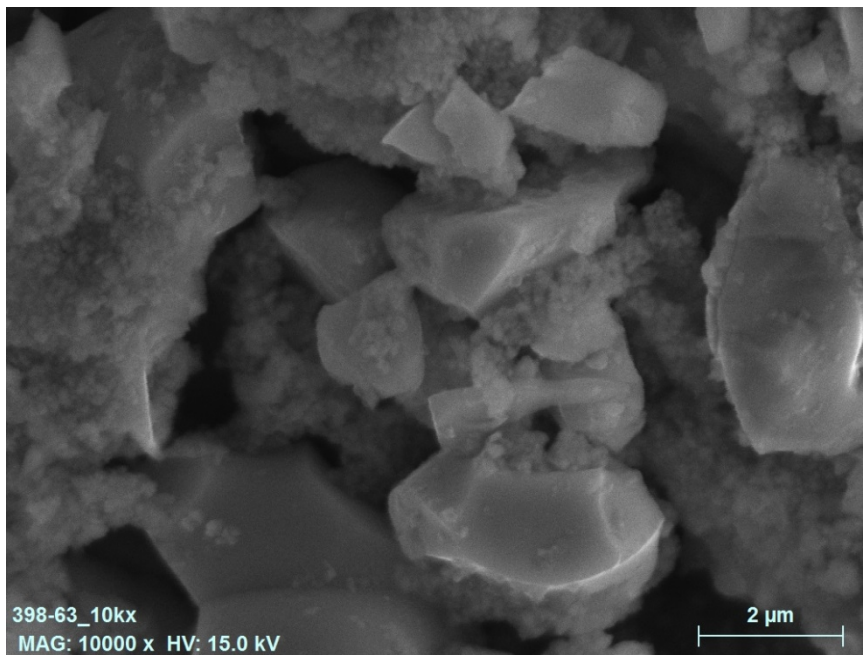


**Figure 10.** SEM micrograph of hetero-coagulated LSCF/LSM (70/30) powder.

### Electrochemical Testing

Two different approaches were pursued for electrochemical characterization of the baseline and core-shell cathode materials: electrochemical impedance spectroscopy (EIS) on symmetrically electrodeed gadolinium doped ceria (GDC) discs and single-cell SOFC testing on large area planar electrolyte supported cells. For all of the cathode materials, screen printing inks were prepared by dispersing appropriate amounts of cathode powder (or constituents of composite cathode powder) into a terpineol based ink vehicle (targeting approximately 75 weight percent solids loading), using a planetary centrifugal (Thinky) mixer. Cathode coatings (15-30 microns thickness) were applied by screen printing and annealed at temperatures ranging from 950 to 1100°C to facilitate adhesion and stabilize microstructure of the coatings.

### EIS Measurements

For EIS measurements, the cathode coatings (1.27 cm diameter) were applied symmetrically on both faces of 2-cm diameter GDC discs (approximately 250 microns thickness). A significant amount of work was performed to improve current collection methods so that reproducible and repeatable EIS measurements could be made. The best results initially were obtained by attaching silver mesh (with pre-attached silver leads) to the electrodes with lanthanum nickel cobaltite (LNC) ink. Even better results were obtained by replacing the LNC ink with non-fritted silver ink. EIS measurements were made over the temperature range of 600 to 800°C with ac amplitude of

180 mV, and frequency range (10  $\mu$ Hz to 300 kHz) that varied with temperature. Examples of Nyquist plots (imaginary versus real parts of impedance) are shown in Figure 11. In these plots, the electrode resistance is calculated as the difference in resistance values where the arcs intersect the x-axis. Area-specific resistance then is calculated from the measured electrode resistance by dividing by two and multiplying by the electrode area. EIS test results obtained during the project are presented and discussed below.

- ❖ An Arrhenius plot of area-specific resistance of the baseline LSCF/GDC formulation is presented in Figure 12. As shown by these data, there is a slight break in the Arrhenius slope at about 500°C, which appears to be consistent with most of the data being collected so far. During this particular test, stable EIS readings could not be obtained at temperatures above 700°C; extrapolation of the data to higher temperatures leads to ASR values of 77 and 32 m $\Omega$ -cm $^2$  at 750 and 800°C, respectively. These ASR values are consistent with those expected for conventional LSCF/GDC cathodes.
- ❖ Arrhenius plots of area-specific resistance of NexTech's standard LSZF/GDC cathode formulation, comparing test results obtained with LNC and silver pastes, are presented in Figure 13. As shown by these data, identical results were obtained by the two methods, which provided confidence in the silver paste based method. The ASR values at 750 and 800°C (13 and 33 m $\Omega$ -cm $^2$ , respectively) are consistent with NexTech's experience. Note that NexTech's standard cathode has two layers, with an active LSZF/GDC layer and a current-carrying pure LSZF layer (and controlled particle size distributions in each layer).

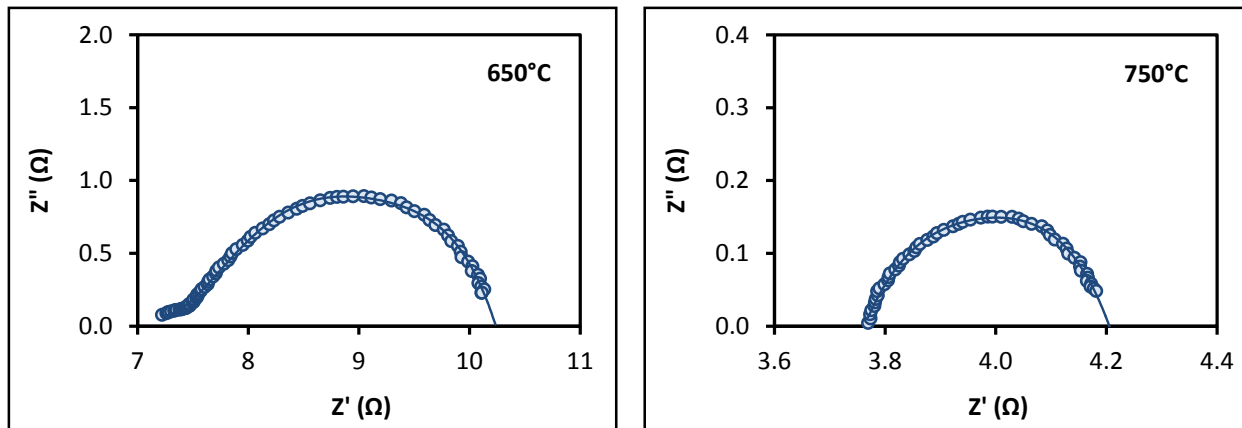


**Figure 11.** Nyquist plots obtained for the baseline LSCF/GDC cathode at 650 and 750°C.

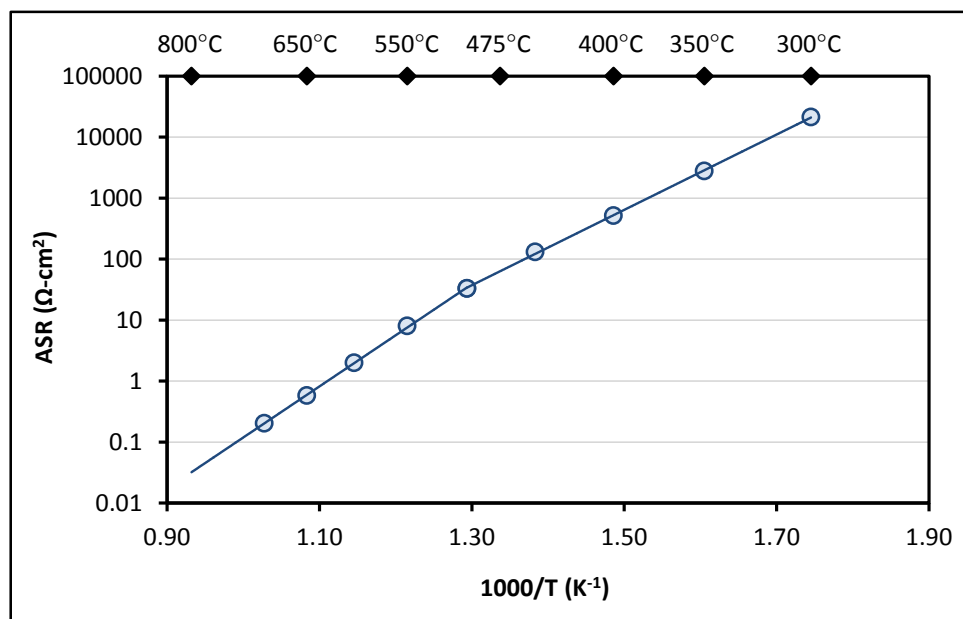


**Figure 12.** Arrhenius plot of area-specific resistance of baseline LSCF/GDC cathode material.

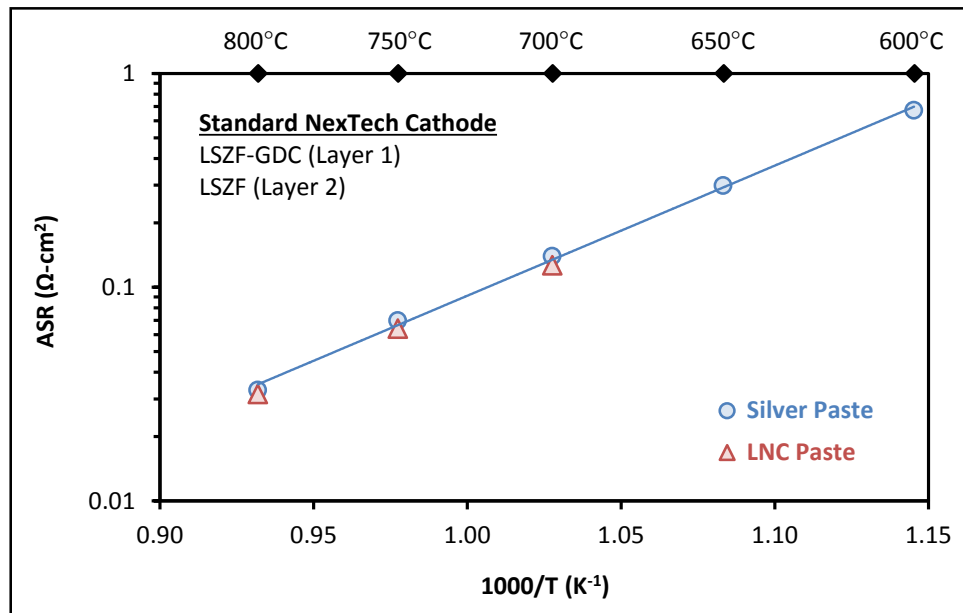


**Figure 13.** Arrhenius plots of area-specific resistance of NexTech's standard LSZF/GDC cathode, comparing current collection methods.

- ❖ Samples were prepared and data were collected, which compare NexTech's standard LSZF/GDC cathodes with "baseline" LSZF/GDC cathodes. Two baseline LSZF/GDC cathodes were made from LSZF ( $5.7 \text{ m}^2/\text{gram}$ ) and GDC ( $5.8 \text{ m}^2/\text{gram}$ ) powders. These were two-layer cathodes, with active LSZF/GDC layers (50 and 68 vol% LSZF) and LSZF current carrying layers. EIS data are presented in Figure 14. As shown by these data, NexTech's

standard LSZF cathode (with optimized particle size distribution) outperforms the baseline LSZF based cathodes, and there was slight change in Arrhenius slope for the baseline LSZF cathodes with different LSZF/GDC ratios in the active layers. When comparing similarly prepared LSCF/GDC and LSZF/GDC cathodes of like composition, slightly better results were obtained with the LSCF/GDC formulation (see Figure 15).

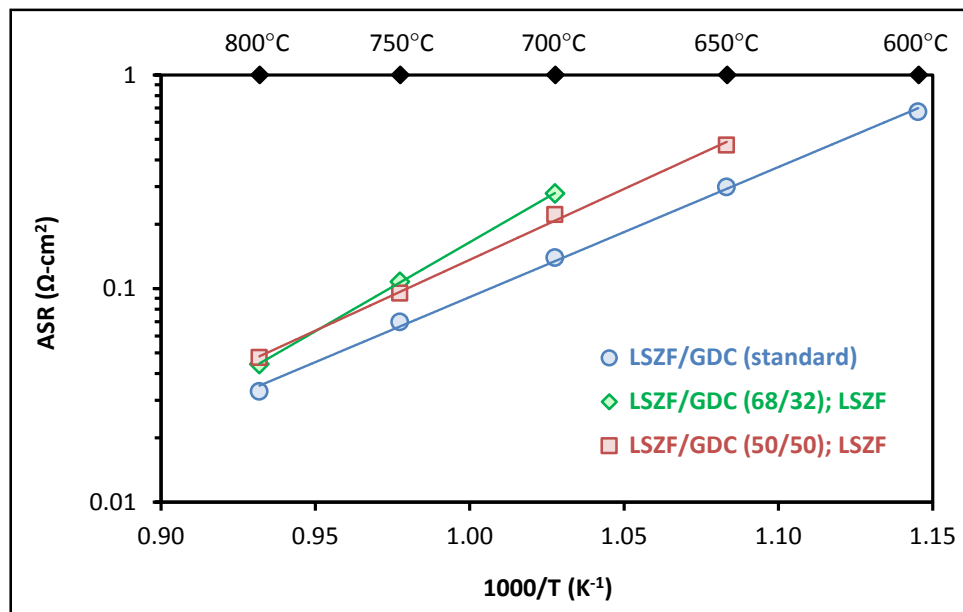


**Figure 14.** Arrhenius plots of area-specific resistance of NexTech's standard LSZF/GDC cathode and two baseline LSZF/GDC cathodes.

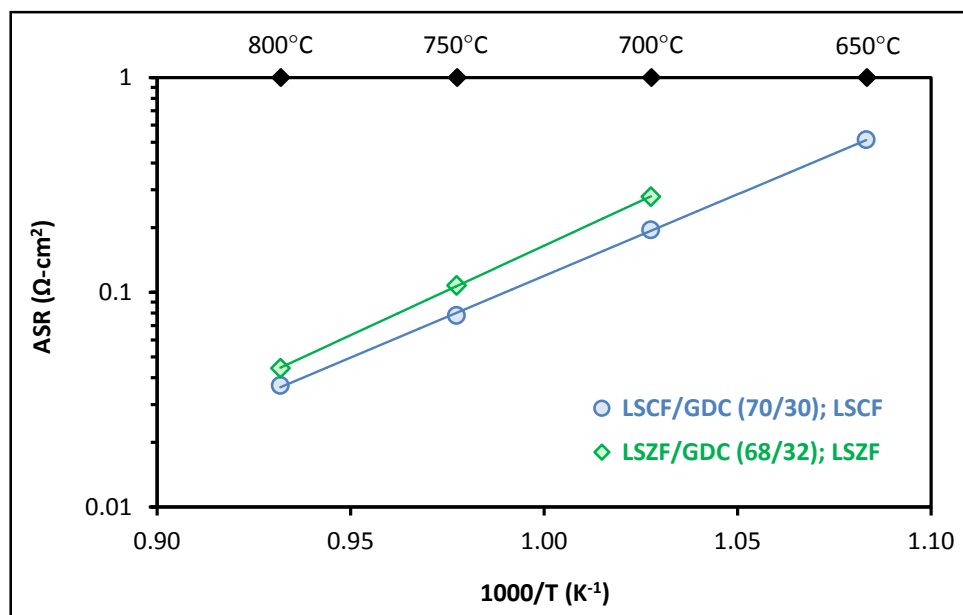


**Figure 15.** Arrhenius plots of area-specific resistance of baseline two-layer cathodes.

- ❖ Cathode-coated GDC disc samples with baseline LSCF (single layer) and LSCF/GDC (dual layer) cathode formulations were made from LSCF ( $5.1 \text{ m}^2/\text{gram}$ ) and GDC ( $5.8 \text{ m}^2/\text{gram}$ ) powders. For the dual layer cathodes, the active cathode layer LSCF/GDC (30 vol% GDC) and the current carrying layer was pure LSCF. As shown by data in Figure 16, the baseline LSCF/GDC cathode was slightly better than the baseline LSZF cathode and the Arrhenius slopes were similar. As shown by EIS data in Figure 16, the dual-layer LSCF/GDC cathodes significantly outperformed the single-layer LSCF cathodes, which is consistent with several literature references.
- ❖ Finally, a cathode-coated GDC disc sample was made with a core-shell LSCF/LSM (70/30) cathode powder made by the hetero-coagulation method. EIS testing results of this core-shell cathode are compared with the single-component LSCF cathode are compared in Figure 17. The results clearly indicate that the single-component LSCF cathode was superior to the LSCF/LSM core-shell cathode.

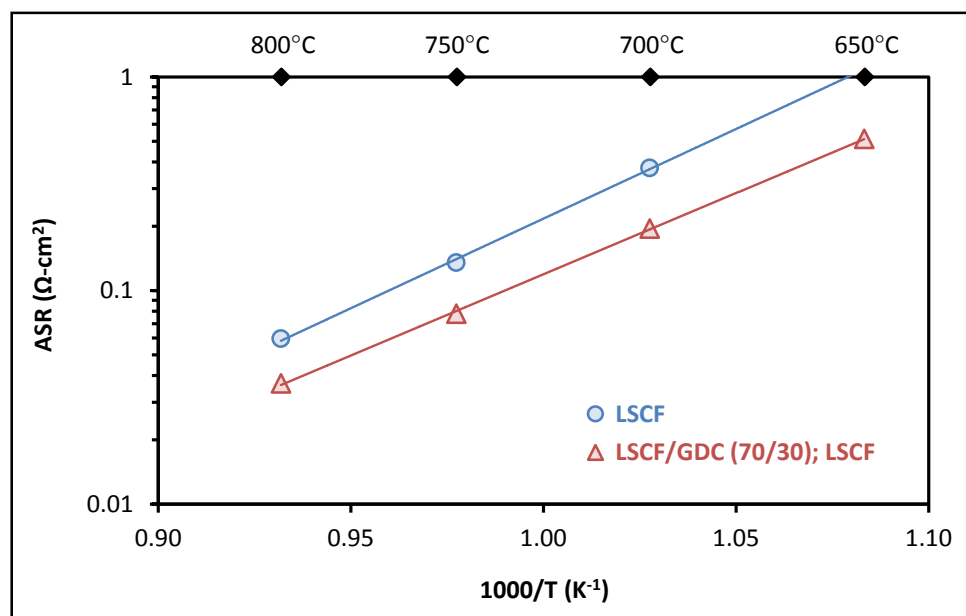


**Figure 16.** Arrhenius plots of area-specific resistance of baseline LSCF and LSCF/GDC;LSCF cathodes.

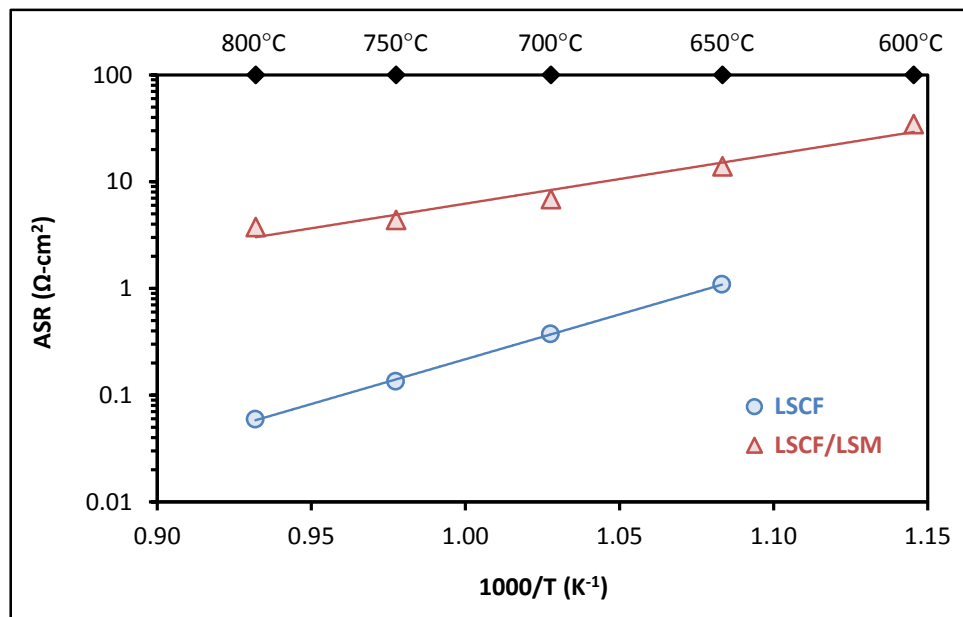


**Figure 17.** Comparison of Arrhenius plots of area-specific resistance for a baseline LSCF cathode and a core-shell (LSCF/LSM) cathode made by the hetero-coagulation method.

### Single-Cell SOFC Testing

Cathode performance and stability also were assessed large-area single-cell SOFC testing of electrolyte supported planar cells (FlexCells) made with scandium stabilized zirconia electrolyte (ScSZ) material. A description of the FlexCell is provided in Exhibit 2, and a schematic of NexTech's single-cell test apparatus is shown in Figure 19. This apparatus enables testing of single cells with the exact same repeat unit configuration as in NexTech's stacks. Also, by attaching a voltage tap to the electrolyte surface on the cathode side of the cell, the cathode voltage drop can be measured. Tests were performed by first heating the cell to 850°C and reducing the anodes according to NexTech's standard protocol, and then collecting polarization curve data at temperatures of 850, 800 and 750°C with a 50/50 (vol%) fuel mixture of hydrogen and nitrogen as fuel (500 sccm total) flowing on the anode and air (1500 sccm) flowing on the cathode. Area-specific resistance (ASR) values were calculated from the slopes of the voltage versus current plots within the voltage range of 0.9 to 0.7 volts. After polarization curves were obtained, the cells were tested under steady state conditions at current densities corresponding to cell potentials of approximately 0.7 volts. Several such tests were performed, with SOFC performance data summarized in Table 5 and long-term testing data summarized in Table 6. The results are described below.

### Exhibit 2. NexTech's FlexCell Platform.

NexTech's SOFC stacks are based on the FlexCell, a patented electrolyte-supported planar cell comprising a thin electrolyte membrane that is mechanically supported by a "honeycomb" mesh of electrolyte material (see Figure 18). More than 60 percent of the active cell area is thin (30 microns), enabling high performance at SOFC operating temperatures of 750 to 800°C. Anodes and cathodes are deposited in separate operations, making it straightforward to incorporate new and improved electrode materials. Although the FlexCell differs from traditional anode supported cells, it shares many of the salient features required for evaluation of core-shell cathode materials.

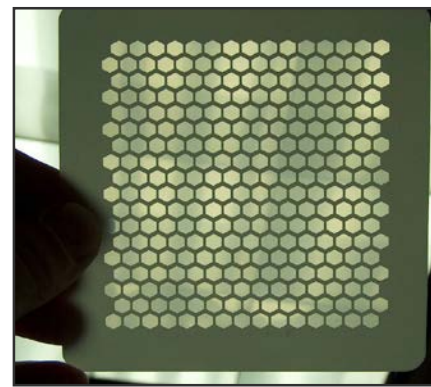


Figure 18. FlexCell membrane.

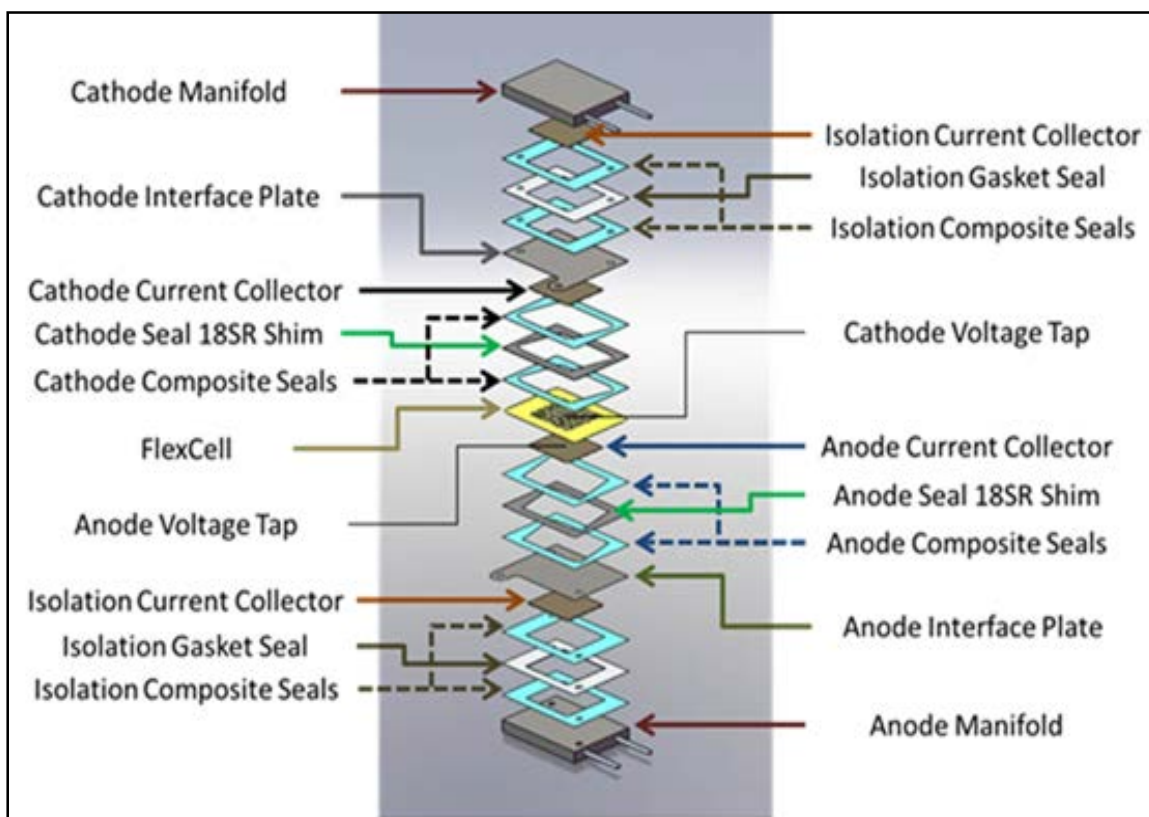
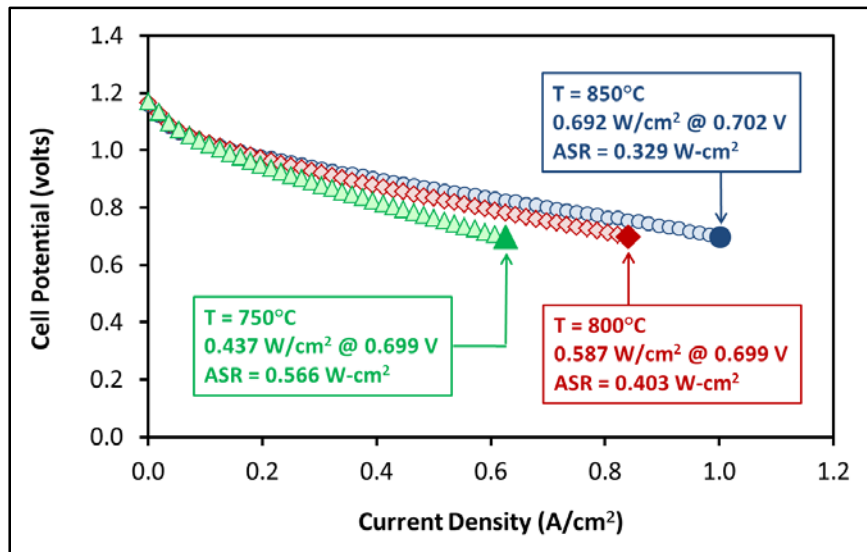


Figure 19. Schematic of NexTech's single-cell testing apparatus.

<b>Table 5.</b> Summary of single-cell SOFC performance data.			
<b>Cathode Formulation (and Process)</b>	<b>Cell ASR Values (<math>\Omega\text{-cm}^2</math>)</b>		
	<b>750°C</b>	<b>800°C</b>	<b>850°C</b>
LSCF (baseline)	0.566	0.403	0.329
LSCF (baseline)	0.736	0.492	0.371
LSZF/GDC (baseline)	0.587	0.426	0.351
LSCF/PSM (80/20) (precipitation process)	1.23	0.781	0.504
LSCF/LSM (70/30) (hetero-coagulation method)	1.15	0.732	0.495

<b>Table 6.</b> Summary of long-term single-cell SOFC testing data.				
<b>Cathode Formulation (and Process)</b>	<b>Test Duration (hours)</b>	<b>Current Density (A/cm<sup>2</sup>)</b>	<b>Cathode Voltage Drop (V)</b>	<b>Cathode Degradation Rate (<math>\mu\text{V/hr}</math>)</b>
LSZF/GDC (baseline)	233	0.59	0.17	17.2
LSCF (baseline)	474	0.47	0.18	59.4
LSCF/PSM (80/20) (precipitation process)	162 193	0.36 0.43	0.25 0.29	25.8 20.1

- ❖ Pole curve data, presented in Figure 20, confirmed that the baseline LSCF cathode provided good cell performance, with total cell ASR values of 0.33, 0.40 and 0.57  $\Omega\text{-cm}^2$  obtained at 850, 800 and 750°C, respectively. These ASR values are comparable to those achieved in previous single-cell tests on ScSZ-based FlexCells at NexTech. A long-term stability test was run under the same fuel and air flows as described above, with a constant current density of 0.57 A/cm<sup>2</sup> and cell temperature of 750°C. The test duration was 250 hours, and data are provided in Figure 21. There was a temporary loss of fuel after about 86 hours of testing, but this event had little impact on the data. As is shown by the data, some deactivation occurred over the first 200 hours of testing, and the rate of this deactivation slowed considerably during the last 50 hours of the test, suggesting a burn-in effect.



**Figure 20.** Polarization curve data for a large-area single cell with baseline LSCF cathode.

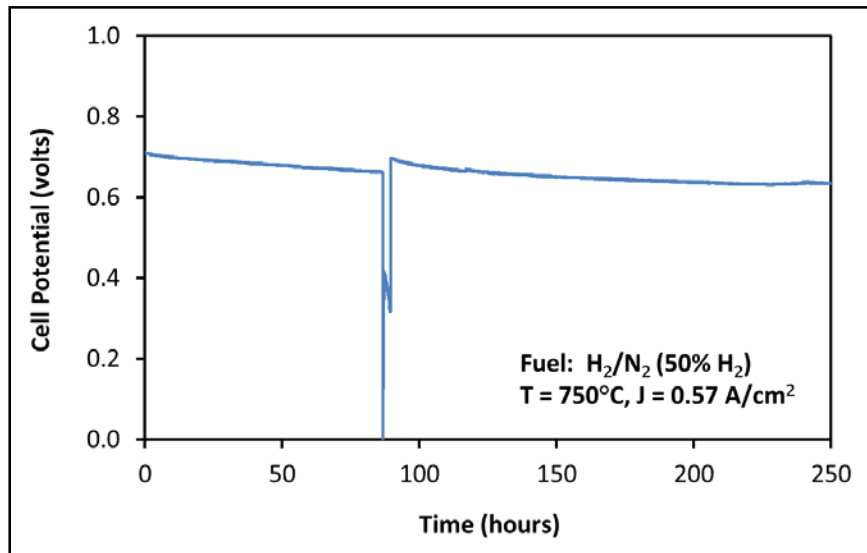


**Figure 21.** Cell potential versus time at 750°C during long-term testing of a cell with a baseline LSCF cathode ( $J = 0.57 \text{ A/cm}^2$ ).

- ❖ A single-cell SOFC test was performed on a cell having a baseline LSCF cathode, with pole curve data presented in Figure 22. Performance of this cell was slightly lower than that of the previous test, which was attributed to anode processing issue during cell manufacturing. For this test, a reference electrode and voltage tap were attached to the electrolyte surface to enable cathode voltage drop and cathode-specific degradation to be determined. Long-term testing results for this cell, with a current density of  $0.47 \text{ A/cm}^2$ , are presented in Figure 23. For this test, the diluted hydrogen fuel was humidified, which significantly reduced the degradation rate observed during the first cell test. However, the cell degradation rate was still fairly high

(74.4  $\mu$ V/hour), which was only slightly larger than degradation measured for the cathode voltage drop (59.8  $\mu$ V/hour). Thus, it was confirmed that fuel humidification reduces cell degradation rate, and that cathode degradation rate of single-component LSCF cathodes is too high for practical SOFC applications (confirming the original premise for this SBIR project).

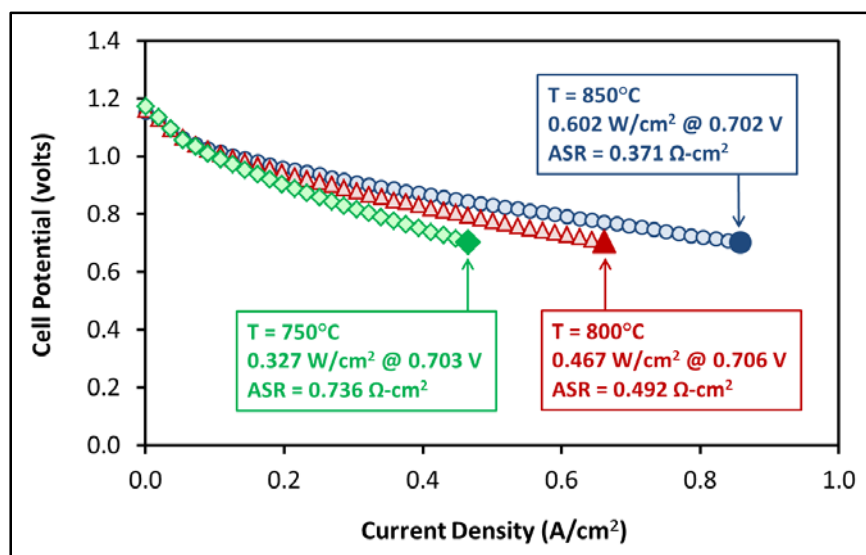


**Figure 22.** Polarization curves obtained for a cell with a baseline LSCF cathode.

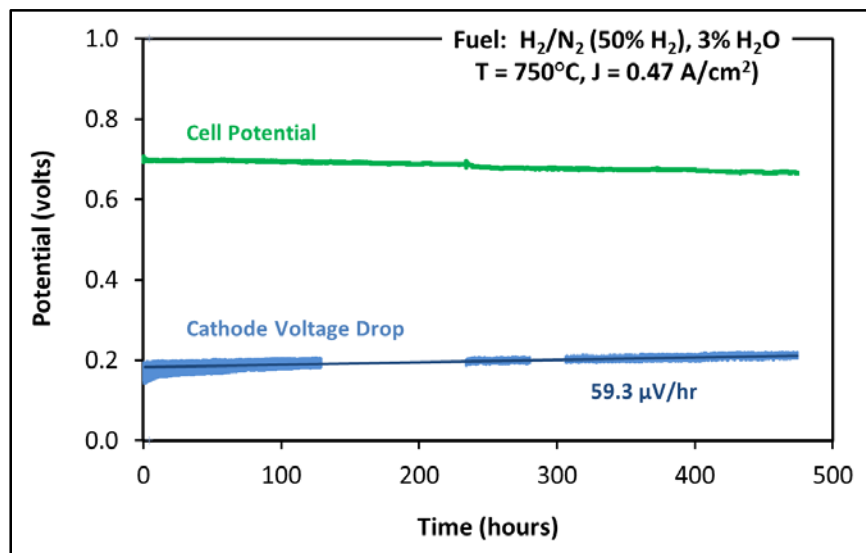


**Figure 23.** Cell potential and cathode voltage drop at 750°C during long-term SOFC testing of a cell with a baseline LSCF cathode ( $J = 0.47$  A/cm<sup>2</sup>).

- ❖ A single-cell SOFC test was performed on a cell having NexTech's standard LSZF-based cathode, with polarization curves presented in Figure 24 and long-term data presented in Figure

25. Performance of this cell was essentially the same as the cell with the baseline LSCF cathode, and the overall degradation rate was similar to that the LSCF cell tested with non-humidified fuel. However, the cathode degradation rate was more than three times lower (17.2  $\mu\text{V}/\text{hour}$ ). Also, during this test, the cell was operated at lower air flow rate (lower air utilization), with the intent of accelerating cathode degradation. However, this had no significant impact on degradation rate.

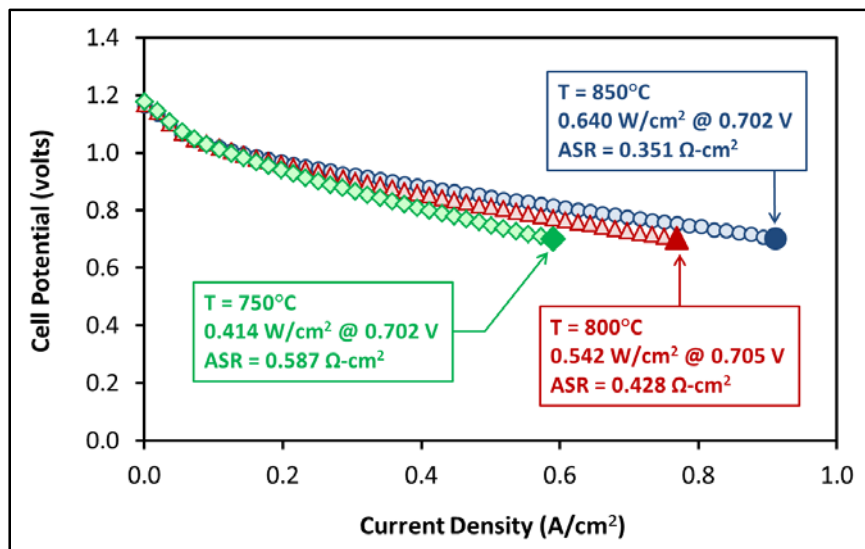


**Figure 24.** Polarization curves obtained for a cell with NexTech's LSZF/GDC cathode.

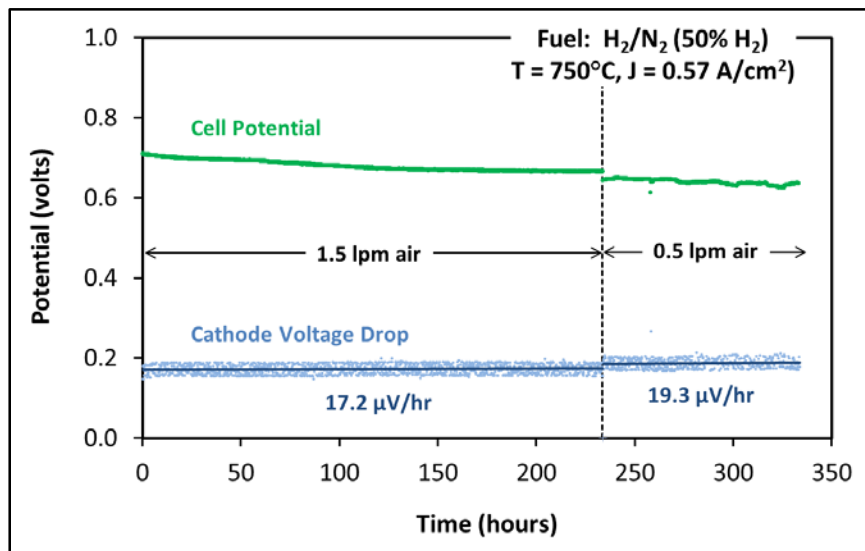


**Figure 25.** Cell potential and cathode voltage drop at 750°C during long-term SOFC testing of a cell with NexTech's standard LSZF/GDC cathode ( $J = 0.57 \text{ A}/\text{cm}^2$ ).

- ❖ Single-cell SOFC tests were performed on cells with core-shell cathodes: LSCF/PSM (80/20) made by the precipitation method and LSCF/LSM (70/30) made by the hetero-coagulation

method. Consistent with previously described EIS data, the performance of these core-shell cathodes was inferior to that of LSCF (see Figures 26-28). A long-term test (with humidified fuel) was performed on the cell with a core-shell LSCF/PSM (80/20) cathode, and these data are presented in Figure 29. The cell degradation was relatively low (consistent with tests performed with humidified fuel), and cathode degradation also was low (20-25  $\mu$ V/hour), although this test was performed with relatively low current densities (0.36 to 0.43  $\text{A}/\text{cm}^2$ ).

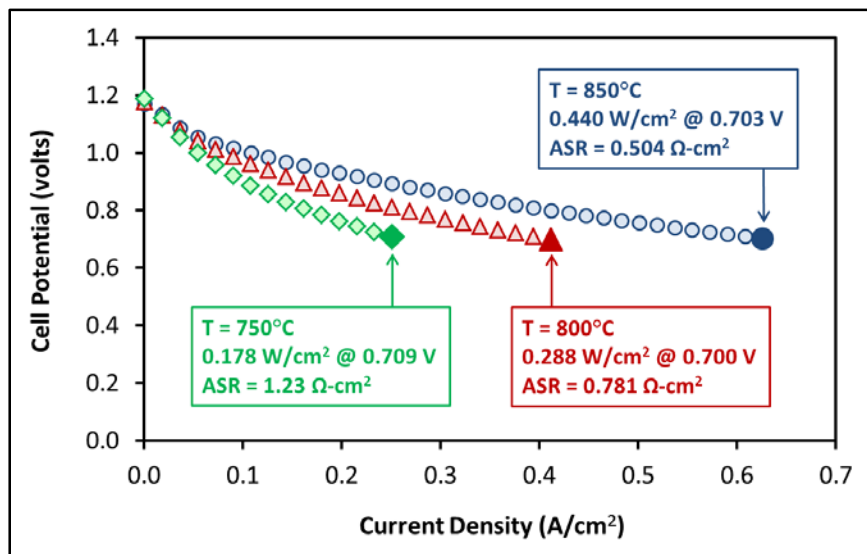


**Figure 26.** Polarization curves obtained for a cell with a core-shell LSCF/PSM (80/20) cathode.

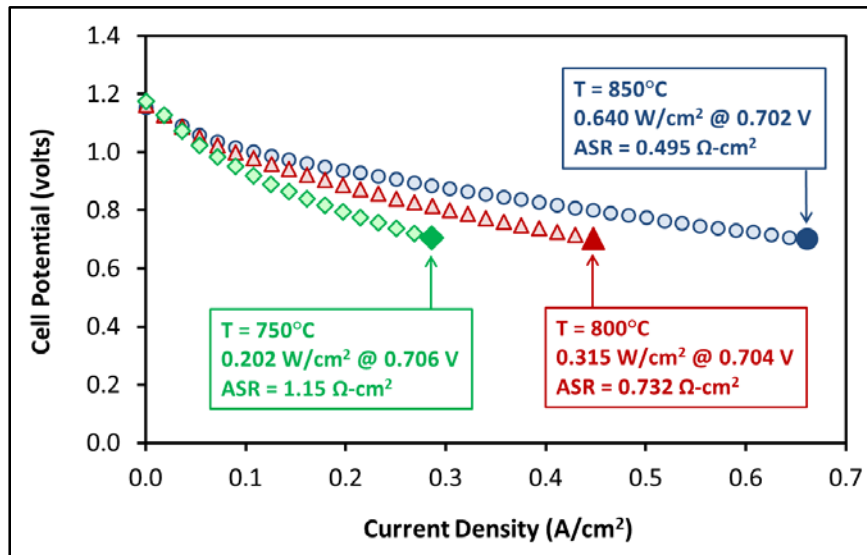


**Figure 27.** Polarization curves obtained for a cell with a core-shell LSCF/LSM (70/30) cathode.

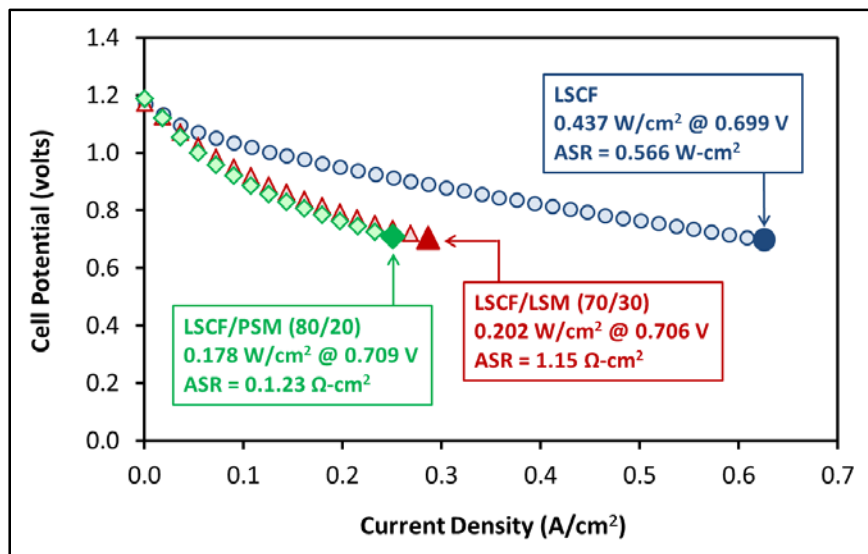


**Figure 28.** Comparison of polarization curves obtained at 750°C for cells with baseline (LSCF) and core-shell (LSCF/PSM and LSCF/LSM) cathodes.

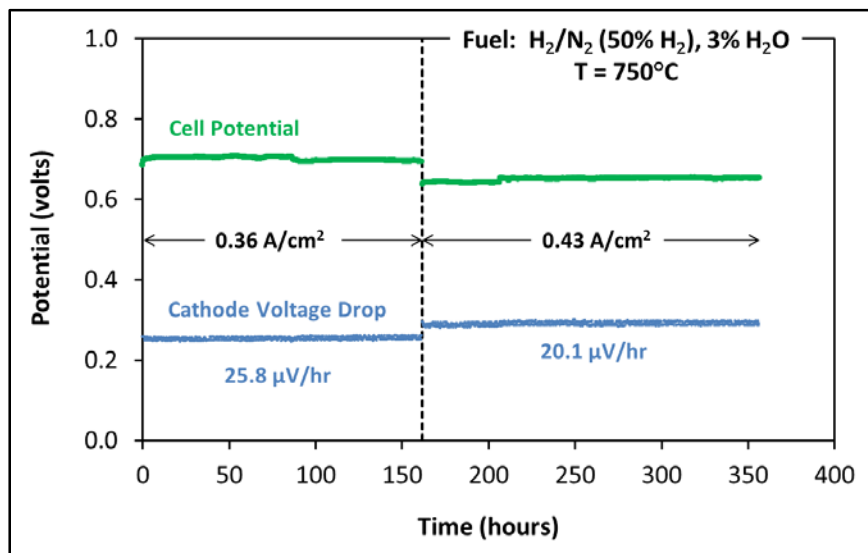


**Figure 29.** Cell potential and cathode voltage drop at 750°C during long-term SOFC testing of a cell with a core shell LSCF/PSM (80/20) cathode made by the hetero-coagulation method.

### **SUMMARY AND CONCLUSIONS**

In this project, a “core-shell” composite cathode approach was evaluated for improving SOFC performance and reducing degradation of LSCF cathodes. It was intended that these core-shell cathode powders that could be dropped into existing SOFC manufacturing processes (e.g., screen printing) rather than adding a processing step (e.g., infiltration).

Ceramic processing methods of milling, precipitation and hetero-coagulation approaches were evaluated for making core-shell composite cathode powders comprised of coarse LSCF “core” particles and nanoscale “shell” particles of LSM or PSM. The targeted core-shell morphology was achieved with the precipitation and hetero-coagulation methods, although perfect coverage of the LSCF core particles by the LSM and PSM particles was not obtained.

Half-cell (EIS) measurements and single-cell SOFC testing was performed to assess performance and durability of the core-shell cathode powders, relative to conventional LSCF-based cathodes. These EIS and SOFC tests conclusively determined that the core-shell cathode powders resulted in significant lowering of performance.

Thus, it was concluded that the core-shell cathode approach did not warrant further investigation.

## **LITERATURE CITED**

- [1] S.P. Jiang, Materials Science and Engineering A **418**, 199–210 (2006).
- [2] S.P. Jiang, International Journal of Hydrogen Energy **37**, 449-470 (2012)
- [3] Z. Jiang, et al, Electrochimica Acta **55**, 3595-3605 (2010).
- [4] Z. Liu, et al., Journal of Energy Chemistry **22**, 555–559 (2013).
- [5] M.E. Lynch, et al., Energy and Environmental Science **4**, 2249-2258 (2011).
- [6] X. Zhu, et al., International Journal of Hydrogen Energy **38**, 5375-5382 (2013).
- [7] M.F. Liu, et al., International Journal of Hydrogen Energy **37**, 8613-8620 (2012).
- [8] P. Hjalmarsson and M. Mogensen, Journal of Power Sources **196**, 7237-7244 (2011).
- [9] A. Samson, et al., Journal of the Electrochemical Society, **158**, B650-B659 (2011).
- [10] A. Samson, et al., Electrochemical and Solid-State Letters **15**, B54-B56 (2012).
- [11] J. D. Nicholas and S. A. Barnett, ECS Transactions **25**, 2435-2442 (2009).
- [12] J. D. Nicholas and S. A. Barnett, Journal of the Electrochemical Society **157**, B536-B541 (2010).
- [13] N. Ai, et al., Journal of the Electrochemical Society **157**, B1033-B1039 (2010).
- [14] X. Lou, et al., Solid State Ionics **180**, 1285–1289 (2009).
- [15] X. Lou, et al., Journal of Power Sources **195**, 419-424 (2010).
- [16] D. Han, et al., Journal of Power Sources **246**, 409-416 (2014).
- [17] L. Meng, Chinese Journal of Catalysis **35**, 38-42 (2014).
- [18] S. Lee, et al., Journal of Power Sources **195**, 118-123 (2010).
- [19] D. Lee, et al., International Journal of Hydrogen Energy **36**, 6875-6881 (2011).
- [20] J.H. Kim and H. Kim, Ceramics International **38**, 4699-4675 (2012).
- [21] H.J. Ko, et al., International Journal of Hydrogen Energy **37**, 17209-17216 (2012).
- [22] M. Shah, et al., Solid State Ionics **187**, 64-67 (2011).
- [23] Y. Zhang, et al., Journal of the Electrochemical Society **160**, F834-F839 (2013).
- [24] S.P. Jiang and W. Wang, Journal of the Electrochemical Society **152**, A1398-A1408 (2005).
- [25] S.P. Jiang and W. Wang, Solid State Ionics **176**, 135-1357 (2005).
- [26] L. Nie, et al., Journal of Power Sources **195**, 4704-4708 (2010).
- [27] L. Xiong, Journal of Rare Earths **28**, 96-99 (2010).
- [28] D. Ding, Journal of Power Sources **196**, 2551-2557 (2011).
- [29] B. Wei, et al., International Journal of Hydrogen Energy **36**, 6151-6159 (2011).
- [30] M.F. Liu, International Journal of Hydrogen Energy **37**, 8613-8620 (2012).
- [31] B. Wei, et al., International Journal of Hydrogen Energy **37**, 13491-13498 (2012).
- [32] T. Klemensø, et al., Solid State Ionics **224**, 21-31 (2012).
- [33] B. Huang, et al., Journal of Power Sources **216**, 89-98 (2012).
- [34] B. Huang, et al., Journal of Power Sources **209**, 209-219 (2012).
- [35] B. Huang, et al., Journal of Power Sources **235**, 20-28 (2013).
- [36] R.W. Wei, et al., Ceramics International **39**, 8411-8419 (2013).
- [37] Y.P. Fu, et al, International Journal of Hydrogen Energy **37**, 19027-19035 (2013).
- [38] T. Garino, Journal of the American Ceramic Society **75** (3), 514-518 (1992).

## APPENDIX A. LITERATURE SURVEY

<b>Review Articles</b>		
<b>Lead Institution:</b> Nanyang Technical University (Singapore)	<b>Lead Author:</b> S.P. Jiang	<b>Citation:</b> Materials Science and Engineering A <b>418</b> , 199-210 (2006)
<b>Article Title:</b> A review of wet impregnation — An alternative method for the fabrication of high performance and nano-structured electrodes of solid oxide fuel cells		
<b>Primary Conclusion(s):</b> Review of wet impregnation as a forerunner to the core/shell concept for anodes and cathodes.		
<b>Lead Institution:</b> Curtin University (Australia)	<b>Lead Author:</b> S.P. Jiang	<b>Citation:</b> International Journal of Hydrogen Energy <b>37</b> , 449-470 (2012)
<b>Article Title:</b> Nanoscale and nano-structured electrodes of solid oxide fuel cells by infiltration: Advances and challenges		
<b>Primary Conclusion(s):</b> Review of wet impregnation for superior anodes and cathodes. Main challenge is long-term stability.		
<b>Lead Institution:</b> University of Science and Technology of China	<b>Lead Author:</b> Z. Jiang	<b>Citation:</b> Electrochimica Acta <b>55</b> , 3595-3605 (2010)
<b>Article Title:</b> Nano-structured composite cathodes for intermediate-temperature solid oxide fuel cells via an infiltration/impregnation technique		
<b>Primary Conclusion(s):</b> Review as of wet impregnation for cathodes with emphasis on two types: infiltrating electrically conductive phase into ionic conducting phase and vice-versa.		
<b>Lead Institution:</b> Politecnico di Milano	<b>Lead Author:</b> R. Pelosato	<b>Citation:</b> International Journal of Hydrogen Energy <b>38</b> , 480-491 (2013)
<b>Article Title:</b> Co-precipitation synthesis of SOFC electrode materials		
<b>Primary Conclusion(s):</b> The article describes the synthesis of $\text{LaMnO}_3$ , $\text{La}_{0.70}\text{Sr}_{0.30}\text{MnO}_{3-\delta}$ , $\text{La}_{0.80}\text{Sr}_{0.20}\text{FeO}_{3-\delta}$ and $\text{La}_{0.75}\text{Sr}_{0.25}\text{Cr}_{0.50}\text{Mn}_{0.50}\text{O}_{3-\delta}$ using a carbonate co-precipitation route in aqueous medium.		
<b>Lead Institution:</b> Nanjing University of Technology (China)	<b>Lead Author:</b> Z. Shao	<b>Citation:</b> Progress in Materials Science <b>57</b> , 804-874 (2012)
<b>Article Title:</b> Advanced synthesis of materials for intermediate-temperature solid oxide fuel cells		
<b>Primary Conclusion(s):</b> Combustion, co-precipitation, hydrothermal, sol-gel and polymeric-complexing processes for making SOFC materials are thoroughly reviewed and parameters relevant to each synthesis process are compared and discussed.		
<b>Lead Institution:</b> Georgia Tech University	<b>Lead Author:</b> M. Liu	<b>Citation:</b> Materials Today <b>14</b> (11), 534-546 (2011)
<b>Article Title:</b> Rational SOFC material design: new advances and tools		
<b>Primary Conclusion(s):</b> Review as of 2011 of new materials and approaches for low temperature SOFCs.		

<b>M. Liu, et al. (Georgia Tech University)</b>		
<b>Lead Institution:</b> Georgia Tech University	<b>Lead Author:</b> D. Ding	<b>Citation:</b> Advanced Energy Materials <b>2013</b> , 1-6 (2013)
<b>Article Title:</b> Efficient electro-catalysts for enhancing surface activity and stability of SOFC cathodes		
<b>Primary Conclusion(s):</b> Infiltration of various cathode materials (lanthanum strontium manganite, praseodymium strontium manganite, and praseodymium strontium cobalt manganite) improves performance and stability of LSCF cathodes.		
<b>Lead Institution:</b> Georgia Tech University	<b>Lead Author:</b> Z. Liu	<b>Citation:</b> Journal of Energy Chemistry <b>22</b> , 555-559 (2013)
<b>Article Title:</b> LSM-infiltrated LSCF cathodes for solid oxide fuel cells		
<b>Primary Conclusion(s):</b> Investigation of LSM-infiltrated LSCF cathodes. Showed improved properties and stability compared to uncoated LSCF.		
<b>Lead Institution:</b> Georgia Tech University	<b>Lead Author:</b> X. Zhu	<b>Citation:</b> International Journal of Hydrogen Energy <b>38</b> , 5375-5382 (2013)
<b>Article Title:</b> Development of $\text{La}_{0.6}\text{Sr}_{0.4}\text{Co}_{0.2}\text{Fe}_{0.8}\text{O}_{3-\delta}$ cathode with an improved stability via $\text{La}_{0.8}\text{Sr}_{0.2}\text{MnO}_3$ -film impregnation		
<b>Primary Conclusion(s):</b> LSM coatings on LSCF core made by one-step drop coating process. Electrodes with coating are superior to LSCF without coatings.		
<b>Lead Institution:</b> Georgia Tech University	<b>Lead Author:</b> M. Liu	<b>Citation:</b> International Journal of Hydrogen Energy <b>37</b> , 8613-8620 (2012)
<b>Article Title:</b> Enhanced performance of LSCF cathode through surface modification		
<b>Primary Conclusion(s):</b> Improved performance using a catalyst (La-Ca co-doped ceria) applied as a shell around an LSCF core. Run for 500 hours with a power density of $1.25 \text{ W/cm}^2$ .		
<b>Lead Institution:</b> Georgia Tech University	<b>Lead Author:</b> J. Kim	<b>Citation:</b> Journal of Materials Chemistry A <b>1</b> , 515-519 (2013)
<b>Article Title:</b> Composite cathodes composed of $\text{NdBa}_{0.5}\text{Sr}_{0.5}\text{Co}_2\text{O}_{5+\delta}$ and $\text{Ce}_{0.9}\text{Gd}_{0.1}\text{O}_{1.95}$ for intermediate-temperature solid oxide fuel cells		
<b>Primary Conclusion(s):</b> Addition of GDC improved performance of $\text{NdBa}_{0.5}\text{Sr}_{0.5}\text{Co}_2\text{O}_{5+\delta}$ cathodes at temperature of $500\text{-}650^\circ\text{C}$ .		
<b>Lead Institution:</b> Georgia Tech University	<b>Lead Author:</b> X. Li	<b>Citation:</b> Energy & Environmental Science <b>7</b> , 306-310 (2014)
<b>Article Title:</b> High-temperature surface enhanced Raman spectroscopy for in situ study of solid oxide fuel cell materials		
<b>Primary Conclusion(s):</b> Raman spectroscopy is a useful tool for probing surface reactions at elevated temperatures. Technique was demonstrated for $\text{SiO}_2$ -coated silver nanoparticles.		
<b>Lead Institution:</b> Georgia Tech University	<b>Lead Author:</b> M. Lynch	<b>Citation:</b> Energy & Environmental Science <b>4</b> , 2249-2258 (2011)
<b>Article Title:</b> Enhancement of $\text{La}_{0.6}\text{Sr}_{0.4}\text{Co}_{0.2}\text{Fe}_{0.8}\text{O}_{3-\delta}$ durability and surface electrocatalytic activity by $\text{La}_{0.85}\text{Sr}_{0.15}\text{MnO}_{3-\delta}$ investigated using a new test electrode platform		
<b>Primary Conclusion(s):</b> LSM-coated LSCF cathodes demonstrated improved performance and durability based on testing of both sputtered model electrodes and functional fuel cells.		

<b>Lead Institution:</b> Georgia Tech University	<b>Lead Author:</b> X. Lou	<b>Citation:</b> Solid State Ionics <b>180</b> , 1285-1289 (2009).
<b>Article Title:</b> Improving $\text{La}_{0.6}\text{Sr}_{0.4}\text{Co}_{0.2}\text{Fe}_{0.8}\text{O}_{3-\delta}$ cathode performance by infiltration of a $\text{Sm}_{0.5}\text{Sr}_{0.5}\text{CoO}_{3-\delta}$ coating		
<b>Primary Conclusion(s):</b> Improving $\text{La}_{0.6}\text{Sr}_{0.4}\text{Co}_{0.2}\text{Fe}_{0.8}\text{O}_{3-\delta}$ cathode performance by infiltration of a $\text{Sm}_{0.5}\text{Sr}_{0.5}\text{CoO}_{3-\delta}$ coating		
<b>Lead Institution:</b> Georgia Institute of Technology	<b>Lead Author:</b> X. Lou	<b>Citation:</b> Journal of Power Sources <b>195</b> , 419-424 (2010)
<b>Article Title:</b> Controlling the morphology and uniformity of a catalyst-infiltrated cathode for solid oxide fuel cells by tuning wetting property		
<b>Primary Conclusion(s):</b> An investigation into the wetting properties of infiltrated catalysts. Controlling the wetting can dramatically improve the uniformity of the catalyst layer and thus improve the performance.		
<b>Lead Institution:</b> Georgia Tech University	<b>Lead Author:</b> L. Nie	<b>Citation:</b> Journal of Power Sources <b>195</b> , 4704-4708 (2011).
<b>Article Title:</b> $\text{La}_{0.6}\text{Sr}_{0.4}\text{Co}_{0.2}\text{Fe}_{0.8}\text{O}_{3-\delta}$ cathode infiltrated with samarium-doped cerium oxide for solid oxide fuel cells		
<b>Primary Conclusion(s):</b> LSCF coated with a thin film of SDC using a one-step infiltration process. This electrode has significant lower polarization resistance and improved stability compared to non-infiltrated LSCF.		
<b>Lead Institution:</b> Georgia Institute of Technology	<b>Lead Author:</b> S. Choi	<b>Citation:</b> www.nature.com Scientific Reports <b>3</b> , 2426; DOI:10.1038/srep02426 (2013)
<b>Article Title:</b> Highly efficient and robust cathode materials for low-temperature solid oxide fuel cells: $\text{PrBa}_{0.5}\text{Sr}_{0.5}\text{Co}_{2-x}\text{Fe}_x\text{O}_{5-\delta}$		
<b>Primary Conclusion(s):</b> Co-doping in a cation-ordered double-perovskite material, $\text{PrBa}_{0.5}\text{Sr}_{0.5}\text{Co}_{2-x}\text{Fe}_x\text{O}_{5-\delta}$ , creates pore channels that dramatically enhance oxygen ion diffusion and surface oxygen exchange while maintaining excellent compatibility and stability. Test cells based on these cathode materials demonstrate peak power densities of $2.2 \text{ W/cm}^2$ at $600^\circ\text{C}$ .		

University of Pennsylvania		
<b>Lead Institution:</b> University of Pennsylvania	<b>Lead Author:</b> Y. Huang	<b>Citation:</b> Journal of The Electrochemical Society <b>151</b> (4), A646-A651 (2004)
<b>Article Title:</b> Fabrication of Sr-doped $\text{LaFeO}_3$ YSZ composite cathodes		
<b>Primary Conclusion(s):</b> Composite LSF/YSZ (40 wt% LSF) cathodes were formed by aqueous impregnation of porous YSZ with La-Sr-Fe nitrate salts followed by calcination. SOFCs prepared with an LSF-YSZ cathode showed improved performance compared to conventional LSM-YSZ cathodes at $700^\circ\text{C}$ .		
<b>Lead Institution:</b> University of Pennsylvania	<b>Lead Author:</b> Y. Huang	<b>Citation:</b> Journal of The Electrochemical Society <b>151</b> (10), A1592-A1597 (2004)
<b>Article Title:</b> Characterization of Sr-doped $\text{LaCoO}_3$ -YSZ composites prepared by impregnation methods		
<b>Primary Conclusion(s):</b> Composite $(\text{La}_{0.6}\text{Sr}_{0.6})\text{CoO}_3$ /YSZ cathodes were formed by aqueous impregnation (as described above). Good performance was achieved but degradation over time was observed.		
<b>Lead Institution:</b> University of Pennsylvania	<b>Lead Author:</b> Y. Huang	<b>Citation:</b> Journal of The Electrochemical Society <b>152</b> (7), A1347-A1353 (2005)
<b>Article Title:</b> Characterization of LSM-YSZ composites prepared by impregnation methods		
<b>Primary Conclusion(s):</b> Composite LSM/YSZ cathodes were formed by aqueous impregnation (as described above) and subjected to electrochemical characterization. Performance was not spectacular.		

<b>Lead Institution:</b> University of Pennsylvania	<b>Lead Author:</b> Y. Huang	<b>Citation:</b> Journal of The Electrochemical Society <b>153</b> (6), A951-A955 (2006)
<b>Article Title:</b> An examination of LSM-LSCo mixtures for use in SOFC cathodes		
<b>Primary Conclusion(s):</b> Co-infiltrated $(\text{La},\text{Sr})\text{MnO}_3$ - $(\text{La},\text{Sr})\text{CoO}_3$ cathodes were not significantly better than infiltrated LSM cathodes, but infiltration of LSCo into LSM/YSZ cathodes provided a substantial performance improvement.		
<b>Lead Institution:</b> University of Pennsylvania	<b>Lead Author:</b> Y. Huang	<b>Citation:</b> Electrochemical and Solid-State Letters <b>9</b> (5), A237-240 (2006)
<b>Article Title:</b> SOFC cathodes prepared by infiltration with various LSM precursors		
<b>Primary Conclusion(s):</b> Composites of LSM and YSZ were prepared by infiltration of LSM nanoparticles, of aqueous salt solutions, and of molten salts into porous YSZ and tested as SOFC cathodes. All of the composites showed essentially identical performance.		
<b>Lead Institution:</b> University of Pennsylvania	<b>Lead Author:</b> W. Wang	<b>Citation:</b> Journal of The Electrochemical Society <b>154</b> (5), B439-B445 (2007)
<b>Article Title:</b> The stability of LSF-YSZ electrodes prepared by infiltration		
<b>Primary Conclusion(s):</b> LSF electrodes were infiltrated into porous YSZ and were tested at 700°C, showing degradation that was attributed to sintering of LSF.		
<b>Lead Institution:</b> University of Pennsylvania	<b>Lead Author:</b> R. Kungas	<b>Citation:</b> Electrochemical and Solid-State Letters <b>13</b> (8), B87-B90 (2010)
<b>Article Title:</b> Doped-ceria diffusion barriers prepared by infiltration for solid oxide fuel cells		
<b>Primary Conclusion(s):</b> An SDC coating was first deposited onto the YSZ scaffold to stabilize subsequently infiltrated $(\text{La},\text{Sr})\text{CoO}_3$ cathodes. The SDC coating prevented solid-state reactions between LSCo and YSZ at 1100°C, which enabled low cathode impedances and acceptable degradation rates to be measured at 700°C.		
<b>Lead Institution:</b> University of Pennsylvania	<b>Lead Author:</b> F. Bidrawn	<b>Citation:</b> Journal of Power Sources <b>195</b> , 720-728 (2010)
<b>Article Title:</b> Dopants to enhance SOFC cathodes based on Sr-doped $\text{LaFeO}_3$ and $\text{LaMnO}_3$		
<b>Primary Conclusion(s):</b> Various dopants ( $\text{Pd}$ , $\text{CeO}_2$ (or SDC), YSZ, $\text{CaO}$ , and $\text{K}_2\text{O}$ ) were incorporated into infiltrated LSM and LSF cathodes via infiltration, and all of these dopants provided performance improvements. The fact that both catalytic and non-catalytic additives improved performance suggests that the improvement is related to structural changes.		
<b>Lead Institution:</b> University of Pennsylvania	<b>Lead Author:</b> F. Bidrawn	<b>Citation:</b> Journal of The Electrochemical Society <b>158</b> (5), B514-B525 (2011)
<b>Article Title:</b> Modeling impedance response of SOFC cathodes prepared by infiltration		
<b>Primary Conclusion(s):</b> A mathematical model was developed to understand the performance of electrodes prepared by infiltration of LSF and LSM into YSZ.		

<b>Nicholas, et al. (Northwestern and Michigan State)</b>		
<b>Lead Institution:</b> Northwestern University	<b>Lead Author:</b> J. Nicholas	<b>Citation:</b> ECS Transactions <b>13</b> (26), 361-377 (2008)
<b>Article Title:</b> Finite element modeling of idealized infiltrated composite solid oxide fuel cell cathodes		
<b>Primary Conclusion(s):</b> A two-dimensional finite element approach was used to calculate the polarization resistance of idealized, branched, nano-particulate, composite cathodes.		

<b>Lead Institution:</b> Northwestern University	<b>Lead Author:</b> J. Nicholas	<b>Citation:</b> ECS Transactions, 25 (2) 2435-2442 (2009)
<b>Article Title:</b> Effect of infiltrate solution additives on samarium strontium cobaltite – cerium gadolinium oxide nano-composite SOFC cathodes.		
<b>Primary Conclusion(s):</b> Nano-composite cathodes were produced by infiltrating SSC nitrate solutions into GDC scaffold layers with various additives. The additives improved phase purity of the infiltrated SSC material, but had little impact on performance.		
<b>Lead Institution:</b> Northwestern University	<b>Lead Author:</b> J. Nicholas	<b>Citation:</b> ECS Transactions <b>28</b> (11), 39-58 (2010)
<b>Article Title:</b> Validation of the simple infiltrated microstructure polarization loss estimation (SIMPLE) model using single layer, nanocomposite $\text{Sm}_{0.5}\text{Sr}_{0.5}\text{CoO}_{3-x}$ – $\text{Ce}_{0.9}\text{Gd}_{0.1}\text{O}_{1.95}$ solid oxide fuel cell cathodes		
<b>Primary Conclusion(s):</b> Polarization resistance measurements of SSC-SDC cathodes showed that the SIMPLE model was able to predict the performance of heavily infiltrated cathodes to within 55 percent at all temperatures from 400-700°C.		
<b>Lead Institution:</b> Northwestern University	<b>Lead Author:</b> J. Nicholas	<b>Citation:</b> Journal of the Electrochemical Society <b>157</b> (4), B536-B541 (2010)
<b>Article Title:</b> Measurements and modeling of $\text{Sm}_{0.5}\text{Sr}_{0.5}\text{CoO}_{3-x}$ – $\text{Ce}_{0.9}\text{Gd}_{0.1}\text{O}_{1.95}$ SOFC cathodes produced using infiltrate solution additives		
<b>Primary Conclusion(s):</b> Nano-composite cathodes were produced in a single infiltration step by infiltrating SSC nitrate solutions into GDC scaffold layers with various additives. The additives improved phase purity of the infiltrated SSC material, but had little impact on performance.		
<b>Lead Institution:</b> Michigan State University	<b>Lead Author:</b> L. Wang	<b>Citation:</b> ECS Transactions <b>35</b> (1), 2321-2329 (2011)
<b>Article Title:</b> Simple infiltrated microstructure polarization loss estimation (SIMPLE) model predictions of today and tomorrow's nano-composite SOFC cathodes		
<b>Primary Conclusion(s):</b> The above SIMPLE model was used to predict the performance of cathodes based on nano-composite mixtures of mixed ionic electron conductors and ion conductors. These predictions agree with the reported values to within 70% or better (without the use of fitting parameters) at all temperatures.		

Lawrence Berkeley National Laboratory		
<b>Lead Institution:</b> LBNL	<b>Lead Author:</b> K. Yamahara	<b>Citation:</b> Solid State Ionics <b>176</b> , 275-279 (2005)
<b>Article Title:</b> Thin film SOFCs with cobalt-infiltrated cathodes		
<b>Primary Conclusion(s):</b> Infiltration of cobalt into an LSM cathode of an anode supported, thin film ScSZ fuel cell led to a significant improvement in SOFC performance.		
<b>Lead Institution:</b> LBNL	<b>Lead Author:</b> K. Yamahara	<b>Citation:</b> Solid State Ionics <b>176</b> , 451-456 (2005)
<b>Article Title:</b> Catalyst-infiltrated supporting cathode for thin-film SOFCs		
<b>Primary Conclusion(s):</b> Infiltration of cobalt into an LSM cathode of a cathode supported, thin film ScSZ fuel cell led to a significant improvement in SOFC performance.		

<b>Lead Institution:</b> LBNL	<b>Lead Author:</b> T. Sholklapper	<b>Citation:</b> Electrochemical and Solid-State Letters <b>10</b> (4), B74-B76 (2007)
<b>Article Title:</b> Synthesis and stability of a nanoparticle-infiltrated solid oxide fuel cell electrode		
<b>Primary Conclusion(s):</b> Nanoparticle LSM catalysts were infiltrated into porous scandia stabilized zirconia electrolyte, forming a cathode that was stable for more than 500 hours at 650°C.		
Lead Institution: LBNL	<b>Lead Author:</b> M. Tucker	<b>Citation:</b> Journal of Power Sources <b>171</b> 477-482 (2007)
<b>Article Title:</b> Performance of metal-supported SOFCs with infiltrated electrodes		
<b>Primary Conclusion(s):</b> Metal-supported SOFCs with thin YSZ electrolyte films and infiltrated Ni and LSM catalysts were made and operated in the temperature range 650–750°C. Infiltration of the electrodes was performed after high temperature brazing operations.		

NETL and West Virginia University		
<b>Lead Institution:</b> NETL	<b>Lead Author:</b> M. Zhi	<b>Citation:</b> ECS Transactions <b>35</b> (1), 2201-2207 (2011)
<b>Article Title:</b> Nanofiber scaffold for solid oxide fuel cell cathode		
<b>Primary Conclusion(s):</b> YSZ and LSM nanofibers were prepared by electrospinning method, characterized, and proposed for use as components of high performance SOFC cathodes.		
<b>Lead Institution:</b> NETL	<b>Lead Author:</b> S. Gandavarapu	<b>Citation:</b> Materials Letters <b>95</b> , 131-134 (2013)
<b>Article Title:</b> Direct foamed and nano-catalyst impregnated solid-oxide fuel cell (SOFC) cathodes		
<b>Primary Conclusion(s):</b> A direct foaming approach was used to fabricate porous LSCF cathodes, and infiltration of platinum nanoparticles were evaluated for electrolyte supported (YSZ) SOFCs. The Pt nano-catalyst impregnated foamed cathode provided better performance than baseline Pt-impregnated LSCF cathode in SOFC tests.		
<b>Lead Institution:</b> NETL	<b>Lead Author:</b> S. Lee	<b>Citation:</b> Journal of the Electrochemical Society <b>158</b> (6), B735-B742 (2011)
<b>Article Title:</b> Effect of Sr-doped LaCoO <sub>3</sub> and LaZrO <sub>3</sub> infiltration on the performance of SDC-LSCF cathode		
<b>Primary Conclusion(s):</b> The effects on performance of commercial SOFC cells with LSCF/SDC cathodes were evaluated for two types of cathode infiltration: a mixed ionic-electronic conductor (La <sub>0.6</sub> Sr <sub>0.4</sub> CoO <sub>3</sub> ) and an electronic insulator (La <sub>1.97</sub> Sr <sub>0.03</sub> Zr <sub>2</sub> O <sub>7</sub> ). LSCo infiltration had a positive impact on cathode performance and LSZ infiltration had a negative influence on performance.		
<b>Lead Institution:</b> West Virginia University	<b>Lead Author:</b> X. Zhang	<b>Citation:</b> Journal of Power Sources <b>269</b> , 412-417 (2014)
<b>Article Title:</b> High performance La <sub>2</sub> NiO <sub>4+δ</sub> -infiltrated (La <sub>0.6</sub> Sr <sub>0.4</sub> ) <sub>0.995</sub> Co <sub>0.2</sub> Fe <sub>0.8</sub> O <sub>3-δ</sub> cathode for solid oxide fuel cells		
<b>Primary Conclusion(s):</b> The electrochemical performance of an LSCF cathode was improved by infiltration of La <sub>2</sub> NiO <sub>4</sub> (LNO). The enhancement of oxygen reduction kinetics was attributed to an increase of active surface area and active reaction regions from heterostructured LSCF/LNO interfaces, and/or favorable cation diffusion from LSCF to LNO.		

<b>Lead Institution:</b> West Virginia University	<b>Lead Author:</b> D. Ding	<b>Citation:</b> Journal of Power Sources <b>196</b> , 2551-2557 (2011)
<b>Article Title:</b> Electrochemical characteristics of samaria-doped ceria infiltrated strontium-doped $\text{LaMnO}_3$ cathodes with varied thickness for yttria-stabilized zirconia electrolytes		
<b>Primary Conclusion(s):</b> Cathodes made of SDC infiltrated into LSM investigated with various cathode thicknesses on YSZ. The best performance was obtained with an electrode thickness of 30 microns.		

Miscellaneous U.S.		
<b>Lead Institution:</b> University of Utah	<b>Lead Author:</b> H. Ding	<b>Citation:</b> Physical Chemistry Chemical Physics <b>15</b> , 489-496 (2013)
<b>Article Title:</b> Suppression of Sr surface segregation in $\text{La}_{1-x}\text{Sr}_x\text{Co}_{1-y}\text{Fe}_y\text{O}_{3-\delta}$ : a first principles study		
<b>Primary Conclusion(s):</b> The problem of strontium surface segregation in LSCF based electrodes was assessed via systematic first principles calculations, which explained the experimental observation that strontium surface segregation is suppressed by LSM coatings on LSCF cathode particles.		
<b>Lead Institution:</b> Northwestern University	<b>Lead Author:</b> S. Shah	<b>Citation:</b> Solid State Ionics <b>187</b> , 64-67 (2011)
<b>Article Title:</b> Time-dependent performance changes in LSCF-infiltrated SOFC cathodes: The role of nano-particle coarsening		
<b>Primary Conclusion(s):</b> Stability studies of electrodes made of GDC infiltrated with LSCF. Observed degradation was attributed to coarsening of the infiltrated LSCF nano-particles.		
<b>Lead Institution:</b> Carnegie Mellon University	<b>Lead Author:</b> R. Chao	<b>Citation:</b> ECS Transactions <b>35</b> (1), 2387-2399 (2011)
<b>Article Title:</b> Preparation of $\text{La}_{0.8}\text{Sr}_{0.2}\text{MnO}_3$ infiltrated coatings in porous SOFC cathodes using evaporation-induced self-assembly		
<b>Primary Conclusion(s):</b> Evaporation-induced self-assembly (EISA) methods were used to infiltrate SOFC cathodes with LSM. A single infiltration step was found to generate thin catalyst coatings through the entire thicknesses of porous YSZ, LSM, and LSCF coatings. The infiltrated LSM coatings were examined using TEM and were shown to be mesoporous.		
<b>Lead Institution:</b> Bucknell University	<b>Lead Author:</b> M. Synodis	<b>Citation:</b> Journal of the Electrochemical Society <b>160</b> (11), F1216-F1224 (2013)
<b>Article Title:</b> A model to predict percolation threshold and effective conductivity of infiltrated electrodes for solid oxide fuel cells		
<b>Primary Conclusion(s):</b> A mechanistic modeling methodology is used to predict both the percolation threshold and effective conductivity of infiltrated SOFC electrodes. The primary model output is the infiltrated electrode effective conductivity which provides results over a range of infiltrate loadings that are independent of the chosen electronically conducting material.		
<b>Lead Institution:</b> Virginia Tech University	<b>Lead Author:</b> K. Lu	<b>Citation:</b> Journal of Power Sources <b>267</b> , 421-429 (2014)
<b>Article Title:</b> Effect of stoichiometry on $(\text{La}_{0.6}\text{Sr}_{0.4})_x\text{Co}_{0.2}\text{Fe}_{0.8}\text{O}_3$ cathode evolution in solid oxide fuel cells		
<b>Primary Conclusion(s):</b> The effect of A/B stoichiometry on interfacial reactions and cathode degradation at 800°C was assessed via SS-441/LSCF/YSZ half-cell structures under electric load. Based on elemental distribution and phase analysis, the evolution of LSCF electrodes and the interaction mechanisms between the LSCF electrodes and the SS-441 alloy are proposed.		

<b>Lead Institution:</b> University of Maryland	<b>Lead Author:</b> E. Wachsman	<b>Citation:</b> ECS Transactions <b>61</b> (1), 47-56 (2014)
<b>Article Title:</b> Towards a fundamental understanding of cathode degradation mechanisms		
<b>Primary Conclusion(s):</b> A fundamental investigation of $H_2O$ and $CO_2$ contaminants in air on cathode degradation mechanisms was performed in order to establish cathode composition/structures and operational conditions to enhance cathode durability.		

<b>Technical University of Denmark (Riso)</b>		
<b>Lead Institution:</b> Technical University of Denmark (Riso)	<b>Lead Author:</b> P. Hjalmarsson	<b>Citation:</b> Journal of Power Sources <b>196</b> , 7237-7244 (2011)
<b>Article Title:</b> $La_{0.99}Co_{0.4}Ni_{0.6}O_{3-\delta}-Ce_{0.8}Gd_{0.2}O_{1.95}$ as composite cathode for solid oxide fuel cells		
<b>Primary Conclusion(s):</b> Infiltration of LSC into a composite cathode material of electronically conducting LCN60 and ionically conducting CGO results in lower electrode polarization than LSM-YSZ. The material was stable at 750°C.		
<b>Lead Institution:</b> Technical University of Denmark (Riso)	<b>Lead Author:</b> A. Samson	<b>Citation:</b> Journal of the Electrochemical Society <b>158</b> (6), B650-B659 (2011)
<b>Article Title:</b> High performance cathodes for solid oxide fuel cells prepared by infiltration of $La_{0.6}Sr_{0.4}CoO_{3-\delta}$ into Gd-doped ceria		
<b>Primary Conclusion(s):</b> Infiltration of LSC from aqueous nitrates into a porous backbone of GDC (prepared by screen printing) provided very low polarization resistances at 600°C.		
<b>Lead Institution:</b> Technical University of Denmark (Riso)	<b>Lead Author:</b> A. Samson	<b>Citation:</b> Electrochemical and Solid State Letters <b>15</b> (4), B54-B56 (2012)
<b>Article Title:</b> Electrodes for solid oxide fuel cells based on infiltration of Co-Based materials		
<b>Primary Conclusion(s):</b> Cathodes made by infiltration of $Co_3O_4$ , $LaCoO_3$ and $La_{0.6}Sr_{0.4}O_{3-\delta}$ from aqueous nitrates into a porous backbone of GDC (prepared by screen printing) were evaluated at 600°C. The best results were obtained with LSC, but there wasn't all that much difference between LSC and $LaCoO_3$ .		
<b>Lead Institution:</b> Technical University of Denmark (Riso)	<b>Lead Author:</b> K. Hanson	<b>Citation:</b> Journal of the Electrochemical Society <b>157</b> (3), 309-B313 (2010)
<b>Article Title:</b> The effect of a CGO barrier layer on the performance of LSM/YSZ SOFC cathodes		
<b>Primary Conclusion(s):</b> The addition of a CGO barrier layer between the electrolyte and the cathode decreases the performance of LSM/YSZ composite electrodes. This was attributed to an increase in series resistance due to bad adhesion of the CGO barrier layer to the YSZ electrolyte.		
<b>Lead Institution:</b> Technical University of Denmark	<b>Lead Author:</b> L. Baqué	<b>Citation:</b> ECS Transactions <b>57</b> (1), 2147-2156 (2013)
<b>Article Title:</b> Enhanced oxygen reduction reaction kinetics in nanocrystalline IT-SOFC cathodes		
<b>Primary Conclusion(s):</b> The increased SOFC performance in nanoscale $La_{0.4}Sr_{0.6}Co_{0.8}Fe_{0.2}O_{3-\delta}$ at 500 to 700°C cannot be solely attributed to an increase of area/volume ratio (higher concentration of active sites for oxygen reduction). A possible explanation was a TEM observation of morphology of nanocrystals surrounded by zones with some degree of crystalline disorder.		

Miscellaneous Europe		
<b>Lead Institution:</b> Forschungszentrum Julich	<b>Lead Author:</b> W. Erning	<b>Citation:</b> Journal of Power Sources <b>61</b> , 205-211 (1996)
<b>Article Title:</b> Catalysis of the electrochemical processes on solid oxide fuel cell cathodes		
<b>Primary Conclusion(s):</b> The addition of low levels of palladium (<0.1 mg/cm <sup>2</sup> ) at the electrolyte surface improves performance of subsequently deposited LSM/YSZ cathodes		
<b>Lead Institution:</b> Imperial College	<b>Lead Author:</b> M. Sahibzada	<b>Citation:</b> Solid State Ionics <b>113–115</b> , 285–290 (1998)
<b>Article Title:</b> Pd-promoted La <sub>0.6</sub> Sr <sub>0.4</sub> Co <sub>0.2</sub> Fe <sub>0.8</sub> O <sub>3</sub> cathodes		
<b>Primary Conclusion(s):</b> The addition of low levels of palladium (up to 15 µg/cm <sup>2</sup> ) via impregnation methods improves performance of LSCF cathodes at low temperatures (550 to 650°C)		
<b>Lead Institution:</b> Queens University (Canada)	<b>Lead Author:</b> E. Hardjo	<b>Citation:</b> Journal of The Electrochemical Society <b>161</b> (1) F83-F93 (2014)
<b>Article Title:</b> An effective property model for infiltrated electrodes in solid oxide fuel cells		
<b>Primary Conclusion(s):</b> An effective property model for infiltrated electrodes is reported that predicts the dependence of effective electronic conductivity and active TPB length on experimentally controllable and measurable parameters.		

S.P. Jiang, et al (Nanyang Technological University and Curtin University)		
<b>Lead Institution:</b> Nanyang Technological University (Singapore)	<b>Lead Author:</b> S.P. Jiang	<b>Citation:</b> Solid State Ionics <b>176</b> , 1351- 1357 (2005)
<b>Article Title:</b> Novel structured mixed ionic and electronic conducting cathodes of solid oxide fuel cells		
<b>Primary Conclusion(s):</b> MIEC cathode material made from LSM impregnated with GDC exhibited improved performance compared to LSM/YSZ or LSM/GDC.		
<b>Lead Institution:</b> Nanyang Technological University (Singapore)	<b>Lead Author:</b> S.P. Jiang	<b>Citation:</b> Journal of the Electrochemical Society <b>152</b> (7), A1398-A1408 (2005)
<b>Article Title:</b> Fabrication and performance of GDC-impregnated (La,Sr)MnO <sub>3</sub> cathodes for intermediate temperature solid oxide fuel cells		
<b>Primary Conclusion(s):</b> Infiltration of GDC into LSM cathodes leads to substantial improvements in cathode performance.		
<b>Lead Institution:</b> Nanyang Technological University (Singapore)	<b>Lead Author:</b> N. Ai	<b>Citation:</b> Journal of the Electrochemical Society <b>157</b> (7), B1033-B1039 (2010)
<b>Article Title:</b> Nanostructured (Ba,Sr)(Co,Fe)O <sub>3-δ</sub> impregnated (La,Sr)MnO <sub>3</sub> cathode for intermediate-temperature solid oxide fuel cells		
<b>Primary Conclusion(s):</b> A nanostructured cathode fabricated by infiltrating BSCF into a porous LSM skeleton exhibited substantially lower electrode polarization resistance compared to pure LSM.		

<b>Lead Institution:</b> Curtin University (Australia)	<b>Lead Author:</b> A. Babaei	<b>Citation:</b> Journal of Alloys and Compounds <b>509</b> , 4781–4787 (2011)
<b>Article Title:</b> Performance and stability of $\text{La}_{0.8}\text{Sr}_{0.2}\text{MnO}_3$ cathode promoted with palladium based catalysts in solid oxide fuel cells		
<b>Primary Conclusion(s):</b> Infiltration of a small amount palladium ( $0.08 \text{ mg/cm}^2$ ) into LSM cathodes greatly reduced polarization resistance of LSM cathodes, and higher Pd levels were detrimental to cathode performance. Co-infiltration of $\text{Pd}_{0.95}\text{Co}_{0.05}$ or $\text{Pd}_{0.8}\text{Ag}_{0.2}$ prevented agglomeration of the infiltrated particles, which improved stability.		
<b>Lead Institution:</b> Curtin University (Australia)	<b>Lead Author:</b> K. Chen	<b>Citation:</b> International Journal of Hydrogen Energy <b>37</b> , 1301-1310 (2012)
<b>Article Title:</b> Enhanced electrochemical performance and stability of $(\text{La},\text{Sr})\text{MnO}_3 - (\text{Gd},\text{Ce})\text{O}_2$ oxygen electrodes of solid oxide electrolysis cells by palladium infiltration		
<b>Primary Conclusion(s):</b> The incorporation of small amount of Pd nanoparticles leads to a substantial increase in electrocatalytic activity and stability of the LSM-GDC oxygen electrodes for hydrogen production via solid oxide electrolysis.		
<b>Lead Institution:</b> Curtin University (Australia)	<b>Lead Author:</b> K. Chen	<b>Citation:</b> International Journal of Hydrogen Energy <b>39</b> , 10349-10358 (2014)
<b>Article Title:</b> Performance and structural stability of $\text{Gd}_{0.2}\text{Ce}_{0.8}\text{O}_{1.9}$ infiltrated $\text{La}_{0.8}\text{Sr}_{0.2}\text{MnO}_3$ nano-structured oxygen electrodes of solid oxide electrolysis cells		
<b>Primary Conclusion(s):</b> The incorporation of GDC nanoparticles via infiltration significantly enhances electrocatalytic activity for oxygen oxidation reaction on LSM electrodes under solid oxide electrolysis cell (SOEC) operating conditions at $800^\circ\text{C}$		
<b>Lead Institution:</b> Curtin University (Australia)	<b>Lead Author:</b> Y. Liu	<b>Citation:</b> International Journal of Hydrogen Energy, article in press (2014).
<b>Article Title:</b> Performance stability and degradation mechanism of $\text{La}_{0.6}\text{Sr}_{0.4}\text{Co}_{0.2}\text{Fe}_{0.8}\text{O}_{3-\delta}$ cathodes under solid oxide fuel cells operation conditions		
<b>Primary Conclusion(s):</b> The performance stability and degradation mechanism of LSCF and cathodes and LSCF impregnated GDC cathodes were investigated under SOFC operation conditions. LSCF and LSCF-GDC cathodes initially showed performance improvement but then degraded grain growth and agglomeration of LSCF, as well as the formation of $\text{SrCoO}_x$ particles on the LSCF particle surfaces.		

<b>Miscellaneous Japan</b>		
<b>Lead Institution:</b> Nippon Telegraph and Telephone	<b>Lead Author:</b> R. Chiba	<b>Citation:</b> Journal of the Korean Ceramic Society <b>45</b> (12), 766-771 (2008)
<b>Article Title:</b> An SOFC cathode composed of $\text{LaNi}_{0.6}\text{Fe}_{0.4}\text{O}_3$ and $\text{Ce}(\text{Ln})\text{O}_2$ ( $\text{Ln} = \text{Sm, Gd, Pr}$ )		
<b>Primary Conclusion(s):</b> The use of Pr-doped ceria, instead of GDC or SDC, led to significantly improved performance of composite LNF/ceria cathodes		
<b>Lead Institution:</b> Nippon Telegraph and Telephone	<b>Lead Author:</b> R. Chiba	<b>Citation:</b> Electrochemical and Solid-State Letters <b>12</b> (5), B69-B72 (2009)
<b>Article Title:</b> SOFC cathodes composed of $\text{LaNi}_{0.6}\text{Fe}_{0.4}\text{O}_3$ and Pr-Doped $\text{CeO}_2$		
<b>Primary Conclusion(s):</b> The use of Pr-doped ceria, instead of GDC or SDC, led to significantly improved performance of composite LNF/ceria cathodes		

<b>Lead Institution:</b> Nihon University,	<b>Lead Author:</b> E. Niwa	<b>Citation:</b> ECS Transactions <b>35</b> (1), 1935-1943 (2011)
<b>Article Title:</b> Low temperature preparation of $\text{LaNi}_{1-x}\text{Fe}_x\text{O}_3$ as new cathode material for SOFC – advantage of liquid phase mixing method		
<b>Primary Conclusion(s):</b> Single phase $\text{LaNi}_{1-x}\text{Fe}_x\text{O}_3$ cathode powders were prepared with low calcination temperature (750°C) with the liquid phase mixing method.		

Miscellaneous Korea		
<b>Lead Institution:</b> Yonsei University (Korea)	<b>Lead Author:</b> S. Lee	<b>Citation:</b> Journal of Power Sources <b>195</b> , 118-123 (2010)
<b>Article Title:</b> LSCF-SDC core-shell high-performance durable composite cathode		
<b>Primary Conclusion(s):</b> A core/shell cathode material was made with LSCF as the shell and SDC as the core using the complex polymerization method. The approach resulted in low polarization resistance and good stability.		
<b>Lead Institution:</b> Yonsei University	<b>Lead Author:</b> D. Lee	<b>Citation:</b> International Journal of Hydrogen Energy <b>36</b> , 6875-6881 (2011)
<b>Article Title:</b> Durable high-performance $\text{Sm}_{0.5}\text{Sr}_{0.5}\text{CoO}_3$ – $\text{Sm}_{0.2}\text{Ce}_{0.8}\text{O}_{1.9}$ core-shell type composite cathodes for low temperature solid oxide fuel cells		
<b>Primary Conclusion(s):</b> A core/shell cathode material was made with SSC as the shell and SDC as the core using the complex polymerization method. It had low polarization resistance and was reasonably stable after 30 temperature cycles.		
<b>Lead Institution:</b> Yeungan University (Korea)	<b>Lead Author:</b> J.H. Kim	<b>Citation:</b> Ceramics International <b>38</b> , 4669-4675 (2012)
<b>Article Title:</b> $\text{Ce}_{0.9}\text{Gd}_{0.1}\text{O}_{1.95}$ supported $\text{La}_{0.6}\text{Sr}_{0.4}\text{Co}_{0.2}\text{Fe}_{0.8}\text{O}_{3-\delta}$ cathodes for solid oxide fuel cells		
<b>Primary Conclusion(s):</b> Cathode materials with a core of GDC and a shell of GDC-supported LSCF and compared to simply-mixed GDC and LSCF. This resulted in low polarization resistance. No stability data was presented.		
<b>Lead Institution:</b> Yonsei University (Korea)	<b>Lead Author:</b> H.J. Ko	<b>Citation:</b> International Journal of Hydrogen Energy <b>37</b> , 17209-17216 (2012)
<b>Article Title:</b> Synthesis and evaluation of $(\text{La}_{0.6}\text{Sr}_{0.4})(\text{Co}_{0.2}\text{Fe}_{0.8})\text{O}_3$ (LSCF) – $\text{Y}_{0.08}\text{Zr}_{0.92}\text{O}_{1.96}$ (YSZ) – $\text{Gd}_{0.1}\text{Ce}_{0.9}\text{O}_{2-\delta}$ (GDC) dual composite SOFC cathodes for high performance and durability		
<b>Primary Conclusion(s):</b> Comparison of two shell/core cathode materials, LSCF/GDC-YSZ and LSCF/YSZ-GDC made with a two-step polymerization method. The LSCF/YSZ-GDC had lower polarization resistance and better stability.		

Miscellaneous Chinese Universities		
<b>Lead Institution:</b> University of Science and Technology of China	<b>Lead Author:</b> X. Zhang	<b>Citation:</b> Journal of The Electrochemical Society <b>160</b> (8) F834-F839 (2013)
<b>Article Title:</b> Microstructural insights into dual-phase infiltrated solid oxide fuel cell electrodes		
<b>Primary Conclusion(s):</b> Numerical techniques were used to construct 3D microstructures of infiltrated electrodes into a porous backbone, and various parameters (such as triple phase boundary length) were assessed.		

<b>Lead Institution:</b> Harbin Institute of Technology (China)	<b>Lead Author:</b> B. Wei	<b>Citation:</b> International Journal of Hydrogen Energy <b>36</b> , 6151-6159 (2011)
<b>Article Title:</b> Nanosized $\text{Ce}_{0.8}\text{Sm}_{0.2}\text{O}_{1.9}$ infiltrated $\text{GdBaCo}_2\text{O}_{5+\delta}$ cathodes for intermediate-temperature solid oxide fuel cells		
<b>Primary Conclusion(s):</b> GBCO was modified by SDC using infiltration techniques was tested as cathode material. The resulting cathode material exhibited low polarization resistance and was stable for 80 hours.		
<b>Lead Institution:</b> Harbin Institute of Technology (China)	<b>Lead Author:</b> B. Wei	<b>Citation:</b> International Journal of Hydrogen Energy <b>37</b> , 13491 – 13498 (2012)
<b>Article Title:</b> Performance evaluation of an anode-supported solid oxide fuel cell with $\text{Ce}_{0.8}\text{Sm}_{0.2}\text{O}_{1.9}$ impregnated $\text{GdBaCo}_2\text{O}_{5+\delta}$ cathode		
<b>Primary Conclusion(s):</b> SOFC tests were completed on anode supported cells with cathodes made by infiltrating SDC into $\text{GdBaCo}_2\text{O}_{5+\delta}$ (with and SDC interlayer). Power density of 790 mW/cm <sup>2</sup> at 700°C with air as oxidant and 1100 mW/cm <sup>2</sup> at 700°C with pure oxygen as oxidant.		
<b>Lead Institution:</b> Huazong University of Science and Technology (China)	<b>Lead Author:</b> L. Meng	<b>Citation:</b> Chinese Journal of Catalysis <b>35</b> , 38-42 (2014)
<b>Article Title:</b> High performance $\text{La}_{0.8}\text{Sr}_{0.2}\text{MnO}_3$ coated $\text{Ba}_{0.5}\text{Sr}_{0.5}\text{Co}_{0.8}\text{Fe}_{0.2}\text{O}_3$ cathode prepared by a novel solid solution method for intermediate temperature solid oxide fuel cells		
<b>Primary Conclusion(s):</b> Synthesized LSM-coated BSCF as a cathode material using a novel solid solution method. Resulted in a low polarization resistance and stable material.		
<b>Lead Institution:</b> Yangtze University (China)	<b>Lead Author:</b> X. Lin	<b>Citation:</b> Journal of Rare Earths <b>28</b> , 96-99 (2010)
<b>Article Title:</b> Effect of samarium doped ceria nanoparticles impregnation on the performance of anode supported SOFC with $(\text{Pr}_{0.7}\text{Ca}_{0.3})_{0.9}\text{MnO}_{3-\delta}$ cathode		
<b>Primary Conclusion(s):</b> SDC was infiltrated into $(\text{Pr}_{0.7}\text{Ca}_{0.3})_{0.9}\text{MnO}_{3-\delta}$ with moderate improvements over other electrodes.		
<b>Lead Institution:</b> Shanghai Institute of Ceramics	<b>Lead Author:</b> D. Han	<b>Citation:</b> Journal of Power Sources <b>246</b> , 409-416 (2014)
<b>Article Title:</b> Nanostructuring of $\text{SmBa}_{0.5}\text{Sr}_{0.5}\text{Co}_2\text{O}_{5+\delta}$ cathodes for reduced-temperature solid oxide fuel cells		
<b>Primary Conclusion(s):</b> Investigation of cathodes produced by infiltrating $\text{SmBa}_{0.5}\text{Sr}_{0.5}\text{Co}_2\text{O}_{5+\delta}$ into porous LSGM scaffold. Results show high power densities.		
<b>Lead Institution:</b> National Dong Hwa University (China)	<b>Lead Author:</b> Y. Fu	<b>Citation:</b> International Journal of Hydrogen Energy <b>37</b> , 19027-19035 (2012).
<b>Article Title:</b> Characterization of nanosized $\text{Ce}_{0.8}\text{Sm}_{0.2}\text{O}_{1.9}$ -infiltrated $\text{Sm}_{0.5}\text{Sr}_{0.5}\text{Co}_{0.8}\text{Cu}_{0.2}\text{O}_{3-\delta}$ cathodes for solid oxide fuel cells		
<b>Primary Conclusion(s):</b> Infiltration of Cu-modified SSC cathodes with SDC increases electrochemical performance.		
<b>Lead Institution:</b> Northeastern University (China)	<b>Lead Author:</b> J. Gao	<b>Citation:</b> Journal of Power Sources <b>218</b> , 383-392 (2012).
<b>Article Title:</b> Substituent effects of $\text{Ba}^{2+}$ for $\text{Sm}^{3+}$ on the structure and electrochemical performances of $\text{Sm}_{0.5}\text{Sr}_{0.5}\text{Co}_{0.8}\text{Fe}_{0.2}\text{O}_{3-\delta}$ cathode for intermediate temperature solid oxide fuel cells		
<b>Primary Conclusion(s):</b> This article describes a chemical synthesis process for Sm-modified BSCF cathode materials. Low polarization resistances and high power densities were obtained at temperatures of 500 to 650°C.		

<b>Lead Institution:</b> National Taiwan University	<b>Lead Author:</b> M. Chen	<b>Citation:</b> ECS Transactions <b>35</b> (1), 2175-2182 (2011)
<b>Article Title:</b> Pr doped ceria and $\text{La}_{0.6}\text{Sr}_{0.4}\text{Co}_{0.2}\text{Fe}_{0.8}\text{O}_3$ composite cathode for solid oxide fuel cell		
<b>Primary Conclusion(s):</b> Cathode performance was improved by using $\text{Pr}_{0.28}\text{Mg}_{0.02}\text{Ce}_{0.7}\text{O}_{2-\delta}$ (instead of GDC) in composite LSCF/ceria cathodes.		
<b>Lead Institution:</b> National Taiwan University	<b>Lead Author:</b> M. Chen	<b>Citation:</b> ECS Electrochemistry Letters <b>2</b> (11), F82-F84 (2013)
<b>Article Title:</b> Theory for the electrical conductivity of nanoparticle-infiltrated composite electrode of solid oxide fuel cell		
<b>Primary Conclusion(s):</b> A new theory for the electronic conductivity was developed based on the physical nature of nanoparticle-infiltrated electrodes and the scaling theory for the percolation threshold of a finite thickness layer. The theory provides a clear explanation for the observed conductivity below the conventional percolation threshold.		
<b>Lead Institution:</b> University of Science and Technology of China	<b>Lead Author:</b> Y. Zhang	<b>Citation:</b> Journal of the Electrochemical Society <b>160</b> (3), F278-F289 (2013)
<b>Article Title:</b> Geometric properties of nanostructured solid oxide fuel cell electrodes		
<b>Primary Conclusion(s):</b> 3D microstructures for nanostructured SOFC electrodes fabricated by infiltration/impregnation method are constructed numerically to enable calculations of key geometric properties at various infiltration loadings, including the percolation probabilities of pores and infiltrated nanoparticles, the total and active three-phase boundary (TPB) length, backbone and nanoparticles surface areas, and backbone-nanoparticles boundary area.		
<b>Lead Institution:</b> Harbin Institute of Technology (China)	<b>Lead Author:</b> B. Wei	<b>Citation:</b> ECS Transactions <b>28</b> (11), 227-233 (2010)
<b>Article Title:</b> Enhanced performance of the $\text{GdBaCo}_2\text{O}_{5+\delta}$ cathode with active $\text{Ce}_{0.8}\text{Sm}_{0.2}\text{O}_{1.9}$ nanoparticles		
<b>Primary Conclusion(s):</b> High performance GBCO/SDC nano-composite cathodes were fabricated by an ion-infiltration method, with active SDC nano-particles (40 nm) forming a continuous ionic-conducting phase on the surface of GBCO backbone, which significantly enhanced the electrocatalytic activity for oxygen reduction reaction.		
<b>Lead Institution:</b> Harbin Institute of Technology (China)	<b>Lead Author:</b> Z. Zhu	<b>Citation:</b> Journal of the Electrochemical Society <b>160</b> (9), F905-F909 (2013)
<b>Article Title:</b> Preparation of LSM-nano-film via a water-based impregnation process and its application onto porous LSCF cathode		
<b>Primary Conclusion(s):</b> A $\text{La}_{0.85}\text{Sr}_{0.15}\text{MnO}_3$ nano-film was prepared onto a porous $\text{La}_{0.6}\text{Sr}_{0.4}\text{Co}_{0.2}\text{Fe}_{0.8}\text{O}_{3-\delta}$ cathode via a water-based impregnation process. The quality of the LSM films were influenced much by drying process, especially relative humidity. The LSM-film reduced interfacial polarization resistance and improved stability of the LSCF cathode at 750°C.		

Core-Shell Battery Materials		
<b>Lead Institution:</b> Beijing Normal University	<b>Lead Author:</b> Y. Li	<b>Citation:</b> Solid State Ionics <b>196</b> , 34-40 (2011)
<b>Article Title:</b> Synthesis and characterization of lithium manganese oxides with core-shell $\text{Li}_4\text{Mn}_5\text{O}_{12}\text{-Li}_2\text{MnO}_3$ structure as lithium battery electrode materials		
<b>Primary Conclusion(s):</b> Lithium manganese oxide composites ( $x\text{Li}_{14}\text{Mn}_5\text{O}_{12}\text{-}y\text{Li}_2\text{MnO}_3$ ) were synthesized by a facile $\text{LiNO}_3$ flux method, using a hierarchical organization precursor of manganese dioxide. The approach improved cycling performance.		

<b>Lead Institution:</b> University of Ulsan (Korea)	<b>Lead Author:</b> J-H Ju	<b>Citation:</b> Journal of Alloys and Compounds <b>509</b> , 7985-7992 (2011)
<b>Article Title:</b> Synthesis and electrochemical performance of $\text{Li}(\text{Ni}_{0.8}\text{Co}_{0.15}\text{Al}_{0.05})_{0.8}(\text{Ni}_{0.5}\text{Mn}_{0.5})_{0.2}\text{O}_2$ with core–shell structure as cathode material for Li-ion batteries		
<b>Primary Conclusion(s):</b> The core-shell structure cathode material $\text{Li}(\text{Ni}_{0.8}\text{Co}_{0.15}\text{Al}_{0.05})_{0.8}(\text{Ni}_{0.5}\text{Mn}_{0.5})_{0.2}\text{O}_2$ was synthesized via a co-precipitation method and its applicability as a cathode material for lithium ion batteries was investigated. Improved performance was observed and improved safety was suggested as a benefit.		
<b>Lead Institution:</b> Institute of Solid State Chemistry (Russia)	<b>Lead Author:</b> N. Kosova	<b>Citation:</b> Solid State Ionics <b>192</b> , 284-288 (2011)
<b>Article Title:</b> From ‘core-shell’ to composite mixed cathode materials for rechargeable lithium batteries by mechanochemical process		
<b>Primary Conclusion(s):</b> A solid state mechanical activation process was applied for surface modification of $\text{LiMn}_2\text{O}_4$ by Li-M-O (M=Co,Co+Ni) and for preparation of composite mixed $\text{LiMn}_2\text{O}_4/\text{LiCoO}_2$ cathode materials. Both the core-shell and composite materials exhibited “superior” electrochemical performance.		
<b>Lead Institution:</b> University of Ulsan (Korea)	<b>Lead Author:</b> S.W. Cho	<b>Citation:</b> Materials Research Bulletin <b>47</b> , 2830-2833 (2012)
<b>Article Title:</b> X-ray absorption spectroscopy studies of the Ni ion of $\text{Li}(\text{Ni}_{0.8}\text{Co}_{0.15}\text{Al}_{0.05})_{0.8}(\text{Ni}_{0.5}\text{Mn}_{0.5})_{0.2}\text{O}_2$ with a core-shell structure and $\text{LiNi}_{0.8}\text{Co}_{0.15}\text{Al}_{0.05}\text{O}_2$ as cathode materials		
<b>Primary Conclusion(s):</b> The core-shell structure cathode material $\text{Li}(\text{Ni}_{0.8}\text{Co}_{0.15}\text{Al}_{0.05})_{0.8}(\text{Ni}_{0.5}\text{Mn}_{0.5})_{0.2}\text{O}_2$ was synthesized via a co-precipitation method and its applicability as a cathode material for lithium ion batteries was investigated. Improved performance and cycling capability was observed.		
<b>Lead Institution:</b> Xiangtan University (China)	<b>Lead Author:</b> X. Yang	<b>Citation:</b> Journal of Power Sources <b>242</b> , 589-596 (2013)
<b>Article Title:</b> Layered $\text{Li}[\text{Ni}_{0.5}\text{Co}_{0.2}\text{Mn}_{0.3}]\text{O}_2\text{-Li}_2\text{MnO}_3$ core shell structured cathode material with excellent stability		
<b>Primary Conclusion(s):</b> A simple sol-gel deposition method was used to synthesize spherical $\text{Li}[\text{Ni}_{0.5}\text{Co}_{0.2}\text{Mn}_{0.3}]\text{O}_2\text{-Li}_2\text{MnO}_3$ core shell composite electrode powder, which exhibited better performance than $\text{Li}[\text{Ni}_{0.5}\text{Co}_{0.2}\text{Mn}_{0.3}]\text{O}_2$ .		
<b>Lead Institution:</b> Tianjin Institute of Power Sources (China)	<b>Lead Author:</b> J. Yu	<b>Citation:</b> Journal of Power Sources <b>225</b> , 34-39 (2013)
<b>Article Title:</b> Solid-state synthesis of $\text{LiCoO}_2/\text{LiCo}_{0.99}\text{Ti}_{0.01}\text{O}_2$ composite as cathode material for lithium ion batteries		
<b>Primary Conclusion(s):</b> A solid state synthesis method was used to fabricate $\text{LiCoO}_2/\text{LiCo}_{0.99}\text{Ti}_{0.01}\text{O}_2$ composite electrodes with core-shell morphology, resulting in greatly improved cycling stability, rate capability, and thermal stability.		
<b>Lead Institution:</b> Anhui University of Technology (China)	<b>Lead Author:</b> C-H. Zheng	<b>Citation:</b> Ceramics International <b>40</b> , 8455-8463 (2014)
<b>Article Title:</b> Synthesis and electrochemical performance of a $\text{LiMn}_{1.83}\text{Co}_{0.17}\text{O}_4$ shell/ $\text{LiMn}_2\text{O}_4$ core cathode material		
<b>Primary Conclusion(s):</b> A shell/core Co-incorporated $\text{LiMn}_2\text{O}_4$ cathode material was synthesized by a facile modified sol-gel process, using highly dispersed $\text{Mn}_3\text{O}_4$ nanoparticles as the Mn source. Electrochemical performance of the shell/core cathode material compared favorably with that of Co-doped doped $\text{LiMn}_2\text{O}_4$ , and rate capability and cycling performance were superior to those of $\text{LiMn}_2\text{O}_4$ made by the same method.		

<b>Lead Institution:</b> Ningbo University (China)	<b>Lead Author:</b> Y. Liu	<b>Citation:</b> Journal of Power Sources <b>256</b> , 66-71 (2014)
<b>Article Title:</b> One-step hydrothermal method synthesis of core-shell $\text{LiNi}_{0.5}\text{Mn}_{1.5}\text{O}_4$ spinel cathodes for Li-ion batteries		
<b>Primary Conclusion(s):</b> Spherical $\text{LiNi}_{0.5}\text{Mn}_{1.5}\text{O}_4$ material with a core-shell structure was synthesized by a urea-assisted hydrothermal method followed by heat treatment with LiOH at high temperature. Superior rate capability and high temperature cycle performance was observed.		
<b>Lead Institution:</b> Central South University (China)	<b>Lead Author:</b> K. Du	<b>Citation:</b> Journal of Power Sources <b>263</b> , 203-208 (2014)
<b>Article Title:</b> A high-powered concentration-gradient $\text{Li}(\text{Ni}_{0.85}\text{Co}_{0.12}\text{Mn}_{0.03})\text{O}_2$ cathode material for lithium ion batteries		
<b>Primary Conclusion(s):</b> A concentration-gradient cathode material with an average composition of $\text{Li}(\text{Ni}_{0.85}\text{-Co}_{0.12}\text{Mn}_{0.03})\text{O}_2$ was synthesized by a co-precipitation method. The electrochemical properties of this core-shell cathode material were found to be far superior than those of the core $\text{Li}(\text{Ni}_{0.9}\text{Co}_{0.1})\text{O}_2$ material.		
<b>Lead Institution:</b> Zhejiang University (China)	<b>Lead Author:</b> G. Xu	<b>Citation:</b> Journal of Power Sources <b>246</b> , 696-702 (2014)
<b>Article Title:</b> Monodispersed $\text{LiFePO}_4@\text{C}$ core-shell nanostructures for a high power Li-ion battery cathode		
<b>Primary Conclusion(s):</b> Monodispersed $\text{LiFePO}_4$ nanopillows were solvothermally synthesized with ethylene glycol, and $\text{LiFePO}_4@\text{C}$ core-shell nanostructures were prepared by a high-yield, facile method. The core-shell nanostructures exhibited good capacity retention and high rate capacity.		
<b>Lead Institution:</b> Tianjin University of Technology (China)	<b>Lead Author:</b> P. Hou	<b>Citation:</b> Journal of Power Sources <b>265</b> , 174-181 (2014)
<b>Article Title:</b> Design, synthesis, and performances of double-shelled $\text{LiNi}_{0.5}\text{Co}_{0.2}\text{Mn}_{0.3}\text{O}_2$ as cathode for long-life and safe Li-ion battery		
<b>Primary Conclusion(s):</b> $\text{LiNi}_{0.5}\text{Co}_{0.2}\text{Mn}_{0.3}\text{O}_2$ was made with a double-shelled structure, and the material exhibited improved cycling capability and thermal stability and excellent rate capability. The improved performance was attributed to the stable and porous outer shell.		
<b>Lead Institution:</b> Tianjin University of Technology (China)	<b>Lead Author:</b> P. Hou	<b>Citation:</b> Electrochimica Acta <b>133</b> , 589-596 (2014)
<b>Article Title:</b> Design, preparation and properties of core-shelled $\text{Li}\{[\text{Ni}_y\text{Co}_{1-2y}\text{Mn}_y]_{(1-x)}\}$ core $\{[\text{Ni}_{1/2}\text{Mn}_{1/2}]_x\}$ shell $\text{O}_2$ ( $0 \leq x \leq 0.3, 6y+3x-6xy=2$ ) as high-performance cathode for Li-ion battery		
<b>Primary Conclusion(s):</b> Core-shelled lithium ion battery cathode materials of the titled composition were synthesized at 800°C from core-shelled precursors obtained via a co-precipitation route. The material exhibited improved cycling capability and thermal stability under severe charge-discharge conditions.		
<b>Lead Institution:</b> Central South University (China)	<b>Lead Author:</b> B. Zhang	<b>Citation:</b> Journal of Power Sources <b>261</b> , 249-254 (2014)
<b>Article Title:</b> Synthesis and characterization of multi-layer core-shell structural $\text{LiFeBO}_3/\text{C}$ as a novel Li-battery cathode material		
<b>Primary Conclusion(s):</b> $\text{LiFeBO}_3/\text{C}$ electrode material was prepared by a spray-drying and carbothermal method. The core-shell structure improved the conductivity and prevented it from air erosion.		

<b>Lead Institution:</b> Tianjin University of Technology (China)	<b>Lead Author:</b> H. Shi	<b>Citation:</b> Journal of Alloys and Compounds <b>587</b> , 710-716 (2014)
<b>Article Title:</b> Core-shell structured $\text{Li}[(\text{Ni}_{0.8}\text{Co}_{0.1}\text{Mn}_{0.1})_{0.7}(\text{Ni}_{0.45}\text{Co}_{0.1}\text{Mn}_{0.45})_{0.3}]\text{O}_2$ cathode material for high-energy lithium ion batteries		
<b>Primary Conclusion(s):</b> Core-shell structured $\text{Li}[\text{Ni}_{0.7}\text{Co}_{0.1}\text{Mn}_{0.2}]\text{O}_2$ displayed remarkably improved cyclability and thermal stability compared with the non-core-shell structured one.		
<b>Lead Institution:</b> Soochow University (China)	<b>Lead Author:</b> H. Ming	<b>Citation:</b> Electrochimica Acta <b>120</b> , 390-397 (2014)
<b>Article Title:</b> Gradient $\text{V}_2\text{O}_5$ surface-coated $\text{LiMn}_2\text{O}_4$ cathode towards enhanced performance in Li-ion battery applications		
<b>Primary Conclusion(s):</b> $\text{V}_2\text{O}_5$ coated $\text{LiMn}_2\text{O}_4$ cathode material was synthesized and characterized. The material exhibited excellent cycling ability and rate capability in lithium batteries – much better than that of uncoated $\text{LiMn}_2\text{O}_4$ .		